OPEN ACCESS Freely available online

PLoS one

Heart Rate Variability Dynamics for the Prognosis of Cardiovascular Risk

Juan F. Ramirez-Villegas[1]*, Eric Lam-Espinosa[2], David F. Ramirez-Moreno[1], Paulo C. Calvo-Echeverry[2], Wilfredo Agredo-Rodriguez[2]

1 Computational Neuroscience, Department of Physics, Universidad Autonoma de Occidente, Cali, Colombia, 2 Engineering Faculty, Department of Automatics and Electronics, Universidad Autonoma de Occidente, Cali, Colombia

Abstract

Statistical, spectral, multi-resolution and non-linear methods were applied to heart rate variability (HRV) series linked with classification schemes for the prognosis of cardiovascular risk. A total of 90 HRV records were analyzed: 45 from healthy subjects and 45 from cardiovascular risk patients. A total of 52 features from all the analysis methods were evaluated using standard two-sample Kolmogorov-Smirnov test (KS-test). The results of the statistical procedure provided input to multi-layer perceptron (MLP) neural networks, radial basis function (RBF) neural networks and support vector machines (SVM) for data classification. These schemes showed high performances with both training and test sets and many combinations of features (with a maximum accuracy of 96.67%). Additionally, there was a strong consideration for breathing frequency as a relevant feature in the HRV analysis.

Citation: Ramirez-Villegas JF, Lam-Espinosa E, Ramirez-Moreno DF, Calvo-Echeverry PC, Agredo-Rodriguez W (2011) Heart Rate Variability Dynamics for the Prognosis of Cardiovascular Risk. PLoS ONE 6(2): e17060. doi:10.1371/journal.pone.0017060

Editor: Kelvin Wong, Royal Melbourne Institute of Technology, Australia

Received November 2, 2010; **Accepted** January 17, 2011; **Published** February 28, 2011

Funding: All the financial resources to carry out this research were provided by Universidad Autonoma de Occidente, Cali, Colombia. They provided the necessary medical equipment for the data recording and analysis. The funders had no role in the preparation of the manuscript.

Competing Interests: The authors have declared that no competing interests exist.

* E-mail: juanfelipe.rv@gmail.com

Introduction

Cardiac diseases are a major cause of mortality in the world. Studies carried out in 2006 in Colombia establish that heart diseases produced circa 30875 deceases with an overall increase of 19.6% since 1999. Therefore, there has been great interest in the development of computational tools for prognosis and diagnosis. The main aim of these tools is to improve performance of cardiologists on prognostic and diagnostic tasks, i.e., reducing both the number of missed diagnoses or prognoses and the time taken to reach such decisions. Under these conditions, it is expected that detecting cardiac signs helps to decrease the mentioned decease rates. At the same time, the introduction of computational systems offers additional benefits, since the early identification of patients would help the specialists to deal efficiently with certain cardiac diseases. Moreover, as traditional risk stratifiers are commonly used for prognosis, their positive predictive value is not as high as the clinical practice demands.

Heart rate variability (HRV) has been often related with the diagnosis and prognosis of certain cardiac diseases and, in fact, is a standard method for studying the autonomic nervous system (ANS) in heart control [1]. Several findings on HRV analysis have demonstrated that geometric, statistical, spectral, multi-resolution and non-linear approaches are powerful tools for the assessment of cardiovascular health [1,2,3,4,5,6,7,8,9,10,11,12,13,14,15,16,17,18]. Several patterns observed from HRV dynamics are often related with myocardial infarction (MI) [18,19], sick sinus syndrome (SSS) [1], multiple cardiac arrhythmias [1], atrial fibrillation (AF) [20], congestive heart failure (CHF) [21], complete heart block (CHB) [2], and ischemic cardiopaty [2], amongst others. Additionally there are some risk factors that affect HRV directly or indirectly, such as blood pressure (BP), alcohol, smoking and drug consumption [2].

Cardiovascular risk in general terms is often related to low or excessive fluctuations of the NN intervals given by intrinsic and extrinsic factors [10]. The relation between reduced HRV and mortality risk was first shown by Wolf et al. in 1977 [22].

Furthermore, during the last 25 years, the significance of HRV in assessing cardiac health has been recognized and various techniques have been developed in order to analyze the fluctuations of NN intervals. Time and frequency domain analyses are often referred to as classical analysis as they were the very first methods being used for the HRV processing [23,24,25,26,27,28,29]; these methods are often inconvenient as they are linear and stationary methods intending to model a highly non-linear phenomenon. These methods as well as visual assessment of the raw HRV data are the most common approaches used in clinical practice.

In 1996, the Task Force of the European Society of Cardiology and the North American Society of Pacing and Electrophysiology (ESC/NASPE) published standards on HRV analysis. They proposed several time and frequency domain parameters and their clinical uses, based on short-term (5 min) and long-term (24 h) HRV data [12,21].

Relatively recent findings have shown that frequency domain methods in HRV are related to hypertension [29]. Subjects with risk factors such as hypertension, obesity, insulin resistance, among others, generally show a high sympathetic activity which is often presented before the clinical manifestation of hypertension. As spectral methods are useful to assess the changes in sympathovagal balance, hypertension has been accurately predicted.

Classical methods of analysis are not absolutely suitable for analysis of HRV [21,30,31,32]. Consequently, some approaches have applied multi-resolution methods to HRV analysis. Multi-resolution methods are related to the wavelet transform multi-level decomposition; given the non-stationarity of the HRV signals [31], the discrete wavelet transform (DWT) and wavelet packet transform calculate the required high and low frequency sub-bands, enabling more accurate HRV analysis. Moreover, wavelet entropy measures have been introduced for the implementation of pattern recognition schemes and seem to provide high performances in diagnosing cardiac diseases [21]. However, to our knowledge, previous work has not considered utilizing wavelet energy measures analysis for HRV assessment.

Recently, new dynamic methods of HRV quantification have been used to uncover nonlinear fluctuations in heart rate that otherwise are not apparent. Several methods have been proposed: Return map (Poincaré plot) calculation [13,14,15,33,34,35,36,37]; Lyapunov exponents/spectrum [2,38]; 1/f slope [39]; approximate and sample entropy (ApEn and SmEn, respectively) [20,40]; and detrended fluctuation analysis (DFA) [41]. Moreover, for the last years these analysis techniques have been useful to understand the HRV dynamics as the response of a highly non-linear system, and therefore to produce discriminative enough features to reach high success rates when several pattern recognition techniques are implemented [2,20]. Pattern recognition in HRV has been used for a variety of applications from prognosis to diagnosis of heart diseases. The most commonly used schemes include: Artificial neural networks (ANN) frames [20]; support vector machines (SVMs) [1,20]; and linear statistical classifiers [21]. In general terms, the performance of these classifiers in prognostic or diagnostic tasks is relatively high (80% to 95% sensitivity in the best cases); however, they have been used for the recognition of several patterns in specific cardiac diseases (e.g., CHF, paroxysmal AF, MI, cardiac arrhythmias, amongst others) rather than for the prognosis of cardiovascular risk.

In this work, HRV analysis methods and pattern recognition schemes (namely, artificial neural networks and support vector machines) were used to discriminate between healthy control subjects and cardiovascular risk patients. Extensive experiments were carried out regarding the overall usefulness of the features with emphasis on the prognostic values associated to classical and non-linear analysis methods. We determined the potential application of such methods to clinical practice in order to increase the success rates of cardiovascular risk assessment. There is a strong consideration for breathing frequency as a relevant feature of the HRV analysis, given the respiratory sinus arrhythmia (RSA) phenomenon [25], [42,43,44]. Additionally, we provide a brief explanation on the implementation of advanced HRV analysis software using the analyses performed in this work and for automatic cardiovascular risk prognosis.

Materials and Methods

1. Ethics Statement

This study was approved by the Institutional Review Board of Universidad Autonoma de Occidente (UAO), Cali, Colombia. Each patient in this study was informed in detail about the procedure and signed an informed consent which guaranteed the transparence of the test and the records' future usage.

2. ECG Database

Two distinct source materials were employed in this study: (a) A database of risk and non-risk individuals given by Coomeva IPS (Health Provider Company) experts and (b) the corresponding electrocardiographic data extracted by us using a medical expert protocol.

The requirement for patient's clinical history and positive or negative cardiovascular risk verification was assessed by Coomeva experts as this verification concedes extreme importance on the validity and quality of the subsequent results of this work. The main purpose of this step was to measure the relationship between HRV indices and the subjects with risk factors. Diabetes Mellitus, high blood cholesterol and other lipids, high blood pressure, metabolic syndrome, overweight, obesity, physical inactivity, tobacco and drug consumption are common risk factors of cardiovascular heart diseases (CHD) and heart failure; nearly all of these risk factors are associated with HRV reduction or excessive fluctuations [45,46,47,48,49]. All the risk subjects (patients) showed at least 3 significant risk factors according to the experts' risk assessment.

In order to get the ECG and respiratory signals, a PowerLab device -ref. ML865- (ADInstruments) and a piezoelectric band -ref. MLT1132/D- were used. PowerLab is a data acquisition system used in a variety of experiments and applications with humans' biopotentials. The unit can record more than 200000 samples per second and has individually selectable input sensibilities. Additionally, it has a bioamplifier (used to record any biological signal from the human body or other source) and an internal processor with low and high pass filters. The hardware of the PowerLab uses the software package Chart and Scope in order to record and analyze each acquired dataset.

On the other hand, a non-invasive blood pressure (NIBP) measure was taken into account for the HRV evaluation as it is considered one of the main risk factors in the cardiovascular assessment [49]. Such measure was extracted by using a multiparameter monitor Spacelabs ref. 90309 which allows us to monitor the following parameters: Electrocardiography, respiration, temperature, non-invasive blood pressure and pulse oximetry.

Each register (a total of 90 electrocardiographic records) was recorded following a medical protocol designed by the teamwork using the frontal-bipolar derivation (D2) of the electrocardiogram. The duration of each record was 5 minutes, following the international standards established by the Task Force of the ESC/NASPE [12]. In addition, the following information was taken from each patient: Age, gender, weight, height, diagnosed cardiovascular diseases, risk valuation given previously (without risk, medium risk or high risk), diagnosed risk factors. All the subjects of this study were in sinus rhythm during the ECG recordings, furthermore, the mean breathing frequency for all was 12.1 ± 2.1breaths/min.

2.1. HRV and Respiratory Sinus Arrhythmia Considerations. Respiration has an important influence in HRV. This phenomenon is known as respiratory sinus arrhythmia (RSA), which is a rhythmic fluctuation of the heart beat intervals in a phase relation with the inspiration and the expiration. The autonomous nervous system (ANS) is the part of the nervous system which extrinsically controls the vital functions and organs such as the heart, lungs and glands. ANS is divided into two major subsystems: The Sympathetic Nervous System and the Parasympathetic Nervous System. These systems are antagonists and responsible for the tuning of some physiologic mechanisms. Intrinsic as well as extrinsic factors may affect such balance and sometimes provoke different nervous activity patterns (sympathetic or parasympathetic), which are often the cause of functional irregularities; those patterns are given by hyper/hypoactivity of such subsystems.

When the respiration is being monitored in a controlled environment, the R-R intervals tend to be shorter during the

inspiration and larger during the expiration. Various theories have been exposed about this phenomenon, according to many experiments on animals [43]. The RSA comes from the control given by the oscillations in the firing rates of the medullar neural networks (central pattern generators, CPGs); the medullar neural network shows periodic oscillations even when the afferent inputs are interrupted. When those oscillations are carried out by afferent stimuli from the receptors in the lungs and the thoracic wall, there is a cardiac rhythm oscillation known as RSA.

Obtaining the respiratory frequency has been used to evaluate the magnitude of the RSA, defined as the sum of the power spectral density estimations on the respiratory band. The variations induced by the respiratory rate introduce a significant change on the measurement of HRV; however, if the respiratory frequency is a constant (i.e., 12 breaths/min) and the tidal volume is relatively constant for the maximum capacity, the error in the measurement caused by respiratory irregularities is eliminated and allows a better stability and an effective comparison of the RSA magnitude between patients [50]. In this study, the above criteria were used to measure HRV in the patients. Consequently, both the recorded ECG signals in resting conditions and specific conditions of the environment were taken into account for the vital signs stabilization.

3. ECG Data Pre-processing

3.1. R-Peak Extraction. The R peaks were extracted using the Pan-Tompkins algorithm and the wavelet transform by keeping the detail coefficients from 2^1 to 2^4 using the Haar wavelet [51].

In order to know the effectiveness of the wavelet decomposition levels, the performance of the algorithm was measured using the detail coefficients from the first decomposition level to the fourth decomposition level using on 6120 heart beats recorded with the implemented medical protocol. The results of this evaluation procedure are summarized in Table 1.

According to Table 1, the most appropriate wavelet decomposition level to extract the R-peak is 2^4, with a sampling frequency of 200 kHz for the ECG signal and using the Haar wavelet. However, the diverse resolution levels on the R-peak extraction procedure may affect the temporal resolution of the signal; thereby a comparison of the estimation of the R-R series was made using the resolutions taken into consideration for this work. We found that, despite the detected false positives, there are no significant spatial and frequency changes on the signal given by the decimation process; thereby, there are no significant variations on the spectral indexes estimation.

3.2. Outlier Removal Procedure. Past publications have shown that eliminating the ectopic HRV data is often better than interpolating them or doing any other cumbersome procedure

Table 1. Performance of the R-peak detection algorithm at various wavelet decomposition levels (sampling frequency of 200 kHz) using the Haar wavelet.

Decomposition Level	FP	FN	Sensitivity (Se - %)	Accuracy (Ac - %)
1	240	270	96.06	91.98
2	220	0	96.53	96.53
3	50	0	99.19	99.19
4	0	0	100.00	100.00

doi:10.1371/journal.pone.0017060.t001

[52]. Grubbs Test extended by Rosner method was used in this work [53,54]. Assuming a normal distribution, Grubbs' outlier test can be used to remove one outlier. Nevertheless, if we decide to remove this outlier, we might be tempted to run Grubbs' test again to see if there is a second outlier in the data; however, the rejection criteria changes. Rosner has extended Grubbs' method to detect several outliers in one dataset. Rosner's several outliers detection method seems to be compatible with HRV signals in general ways [54].

For a specified limit k of the number of outliers, the procedure is calculated by using reduced samples of length $n, n-1, ..., n-k+1$, respectively. For each sample $(n-i)$:

$$R_i = \frac{(\max|x_j - \bar{x}|)}{s}, \text{ for } i = 0, 1, 2 \ldots k. \quad (1)$$

where $\bar{x}$ is the mean and s is the standard deviation of the sample $(n-i)$ and j is the position of one given value of the sample. In this way, the critical values of the test are determined by specifying α and by calculating β and $\lambda(\beta)$ in order to calculate the t-student statistical test [53].

4. HRV Classical Measures

4.1. Statistical or Time-domain Measures. In this approach, a set of 7 well-known statistical indexes were calculated: First, the mean and the standard deviation (SDNN) of the NN intervals of each 5 min record; second, the square root of the mean of the sum of the square of differences between adjacent NN intervals (RMSSD); third, the so-called pNN50 was computed as the NN50 count value divided by the total of all NN intervals, where NN50 is the count of adjacent intervals differing by more than 50 ms in the entire HRV record; fourth, the interquartile margin of the NN intervals (MIRR) was also calculated, i.e., the first quartile subtracted from the third quartile of the NN series; in addition, the median of the absolute differences of the NN intervals (MDARR) and the standard deviation of the differences between adjacent NN intervals (SDSD) were calculated.

4.2. Spectral or Frequency-domain Measures. Spectral or frequency-domain measures are based on the power spectral density (PSD) analysis of the R-R series. In this kind of analysis some processing techniques, such as interpolation and detrending, are necessary. The spectral measures have the advantage of relating the power of variation in different frequency bands to different physiological modulating effects [2,24]. Extensive experiments have shown that parametric methods (AR spectrum) tend to produce better results than classical nonparametric methods (Welch's periodogram) when the data length of the signal is relatively short, as is the case with HRV data [20]. For this reason, we applied parametric PSD estimation. Three main spectral measures are distinguished from the spectrum of the R-R series: The power of the very low frequency band (VLF band, 0–0.04 Hz), the power of the low frequency band (LF band, 0.04–0.15 Hz) and the power of the high frequency band (HF band, 0.15–0.4 Hz). These frequency components and their normalized values (NLF and NHF) were calculated using a standard integration procedure (area under the curve) of the spectrum regions. In addition, the ratio of LF to HF was calculated as it indicates the balance of ANS.

For parametric spectral methods, the data can be modeled as the output of a discrete and causal filter whose input is white noise.

The spectral power of an AR process is given by:

$$\hat{P}_{AR}(f) = \frac{1}{f_s}\left|1 + \sum_{k=1}^{p} \hat{a}_p(k)\exp\left(\frac{-2\pi jkf}{f_s}\right)\right|^{-}, \quad (2)$$

where $a(k)$ are the recursive coefficients calculated by covariance method [2]. An important factor in the implementation of the AR method is the selection of the order [28]. The order $p = 16$ for the AR model was taken into account for this study [26,54,55].

5. Wavelet Packet Measures

According to the literature consulted [21], there is a three step procedure to calculate the wavelet measures: First, calculate the wavelet packet coefficients; second, calculate the wavelet energy; and third, calculate the wavelet entropy.

The wavelet packet analysis in HRV is used to separate the signal into multiple scales. This method allows us to analyze both frequency and spatial domains and removes polynomial non-stationarities of the signal [11]. Due to this property, wavelet analysis is much more suitable for analyzing HRV signals than statistical and spectral methods. In this work, the wavelet packet analysis was implemented by using the DB4 function as mother wavelet [21]. The decomposition was performed at a level of 5 [21,56,57].

Once the wavelet coefficients are known, it is possible to calculate the energy for each coefficient:

$$E_j = (C_j)^2. \quad (3)$$

Then, the total energy can be calculated as the mean value of the energy for each coefficient.

On the other hand, the wavelet entropy can be calculated as the probability distribution of the coefficients or the wavelet energy into normalized values:

$$p_j = \frac{E_j}{E_{total}}. \quad (4)$$

In this way, using the definition of entropy given by Shannon, the entropy can be calculated as follows:

$$WS = -\sum_j p_j \log_2(p_j). \quad (5)$$

In [21], the wavelet entropy is calculated as a unique multi-resolution measure. However, in this work, both the energy and entropy measures are taken into account due to their high cardiovascular risk prognostic value.

A problem with wavelet packets implementation is coping with redundant information coming from the wavelet transform computation for the approximation and detail coefficients [54]. In order to avoid the redundant information due to wavelet packet decomposition, a standard Principal Component Analysis (PCA) was computed. PCA chooses a dimensionality reduction by linear projection that maximizes the scattering of all projected samples. The resultant feature space is the projection of the original data set over the covariance matrix eigenvectors, which constitutes the weights of each feature on the input space according to how much of the model's variability is explained by them. The most important entropy and energy features (in terms of variability) were selected.

6. Non-Linear Measures

HRV has been often evaluated using non-linear methods [6,20,58]. These methods seem to be very relevant in feature extraction of the HRV series; on the other hand, HRV dynamics is highly non-linear and, actually, HRV series is the response of a chaotic system, i.e., a system with high sensitivity on the initial conditions [59,60,61].

6.1. Poincaré Map-Based Features. The most popular non-linear technique to assess the HRV is the so-called Poincaré map (also called return map or Lorenz map). The Poincaré map corresponds to the reconstruction of the attractor of the system based on the HRV experimental series [60]. This map can be constructed by plotting each RR interval against the next interval. This plot is very useful in summarizing beat-to-beat information on heart behavior. The Poncaré plot is a simple visual interpretation technique and it has proved to be a very powerful predictor of disease and cardiac dysfunction [21].

In order to extract features of the Poincaré map, two methods were applied in this work: The ellipse fitting technique and the histogram technique [17].

A group of axes with orientation onto the identity line or principal diagonal is the main feature of the ellipse fitting technique. The axes of the plot are related to a new group of axes with a rotation of $\pi/4$ [17].

On the new reference system axes, the dispersion of the points through the x_1 axis is measured by its standard deviation, denoted SD1. On the other hand, the magnitude of the points through the identity line shows the level of long term variability, denoted SD2, i.e., the standard deviation over the x_2 axis.

On the other hand, the ellipse approximation is satisfactory in many cases; however, the shortening that occurs on short R-R intervals is not taken into account by this technique [35]. The histogram approximation has been used to evaluate the distribution of the data into several time ranges. There are three types of histograms: The width histogram, the NN interval histogram and the length histogram [17].

As the visual interpretation of the histogram can be useful to extract information about the heart, it is necessary to parameterize it. The computation of the width of the three histograms is a very strong feature for the prognosis of cardiovascular risk, as it gives the absolute statistical ranges of the NN intervals and its projections. These features are useful for assessing short term HRV, long term HRV and the distribution of NN intervals itself. These histogram widths were taken into account in this study.

6.2. Complexity Analysis. There are several approximations for estimating regularities of different kinds of signals. The most widely used complexity measures for short and noisy data series are approximate entropy (ApEn) and sample entropy (SmEn). These features assign a non-negative number to temporal series in order to quantify the regularity of its fluctuations. Given this fact, complexity measures have been highly useful for the analysis of HRV signals [20].

To calculate ApEn and SmEn from temporal series it is necessary to choose two parameters: A length m and a window size r. ApEn measures the logarithmic similarity amongst neighboring input patterns (those with a separation radius less than r) for m contiguous observations. On the other hand, SmEn is an unbiased estimator introduced to avoid the self-couplings and to quantify the regularity of highly irregular temporal series. SmEn is equal to

the negative of the natural logarithm of a conditional probability. It is the probability that sequences close to each other for m consecutive data points will also be close to each other when one more point is added to each sequence [20].

For both, ApEn and SmEn calculation, it is recommended to take $r=k\sigma$, where σ is the standard deviation of the data series and k runs over 0.1 to 0.2 [62] (for details regarding the calculation of complexity analysis measures see Appendix S1).

7. Statistical Significance Tests and Feature Selection

Up to this moment, several statistical methods have been related to feature selection for training and testing classifiers and for improving their overall performance. As most of computational methods in pattern recognition require a feature selection step, the nature of such procedure depends largely on the structure of the data. As a result, many computational approaches use parametric statistics, e.g., the so-called multivariate analysis of variance (MANOVA), which often reports adequate results for such purposes. However, we cannot assume that all the data has resemblance to a standard normal distribution at high statistical significance. Therefore, we implemented two methods in order to test the normality of the data: First, we conducted the Pearson's chi-square test; and second, the one-sample KS-test. According to our results, the data (for all the features taken into account), has a remarkably different distribution when compared to the normal distribution (with $p<10^{-9}$). As both methods reported quite similar results, we concluded that non-parametric (distribution-free) statistical methods needed to be implemented at this stage. These methods, unlike parametric statistics, make no assumptions about the probability distributions of the variables being assessed. Figure 1 depicts the empirical cumulative distribution plot for a given feature (note the significant difference to the standard normal distribution).

Statistical significance of these results was tested using a standard two-sample KS-test. A level $p<0.05$ was considered a statistically significant difference [63]. On the other hand, in order to use the best features on the classification stage, a level $p<0.0001$ was considered statistically relevant enough as KS test-based selection criteria.

8. Classification

Multilayer Perceptrons (MLP), Radial Basis Function (RBF) networks and several Support Vector Machines (SVM) were evaluated for the classification stage of this work. All classification schemes were trained to capture the difference between cardiovascular risk subjects and healthy ones.

8.1. Multi-layer Perceptron (MLP) Neural Network. Multilayer Perceptrons (MLP) are frequently implemented for classification tasks, given their generalization capabilities. In this work, a standard three-layer network has been proposed.

Let $\mu\,(x_i^\mu)$ be an input pattern, the output of a single artificial neuron of the hidden layer is given by the following equation:

$$Y_j^\mu = f_j\left(\sigma_j^\mu\right) = f_j\left(\sum_{i=1}^{N} w_{ji}^\mu * x_i^\mu + \theta_j\right), \tag{6}$$

where w_{ji}^μ is the synaptic weight i of the neuron, θ_j is the bias and f_j is the activation function. In the current model we have two non-linear transfer functions corresponding to the hidden and the output layers, given by the following equations, respectively.

$$f_j(x) = \frac{\exp(x)-\exp(-x)}{\exp(x)+\exp(-x)}. \tag{7}$$

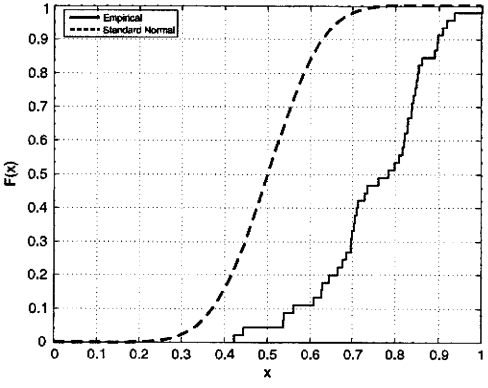

Figure 1. Cumulative distribution plots comparison between a given feature considered in this work and the standard normal distribution.
doi:10.1371/journal.pone.0017060.g001

$$f_k(x) = \frac{1}{1+\exp(-x)}. \tag{8}$$

This architecture guarantees that the network's output will run over 0 and 1 (given the sigmoid output function).

We used the Levenberg-Marquardt backpropagation algorithm to train the MLP neural network, as it is the most popular and successful learning method for training MLPs. The algorithm employs iterative mean squared error minimization using least squares curve fitting [64].

The network consisted of three layers (the sensory input layer, the hidden layer and the output layer), with 5, 200 and 1 neurons, respectively.

8.2. Radial Basis Function (RBF) Neural Network. RBF network is a well-known classifier which combines supervised and unsupervised learning. A standard three-layer RBF network was implemented in this work. The hidden layer of the network is responsible for producing a non-linear expansion of the input space to a hidden space where the classes are linearly separable by unsupervised learning [64]. The most popular unsupervised learning rule for the hidden layer is the so-called k-means.

In this procedure, we establish a number of neurons (k), whose synaptic weights w_{ji} are randomly distributed on the input space and then a similarity measure is calculated, i.e., the Euclidean distance.

When this procedure is applied to the whole layer, the weight update rule is then calculated from:

$$\hat{w}(t+1) = \frac{1}{N_i}\sum_{i=1}^{Ni} \hat{x}_i, \tag{9}$$

where N_i is the number of input vectors associated to each Gaussian node of the hidden layer. This procedure is computed until the stabilization of the synapses is reached (the weights do not change from a training cycle to another).

The Gaussian scale parameters for each hidden neuron can be determined by the approximated magnitude of the influence radius of each neuron on the input space in relation to other neurons near to the j neuron.

This network consisted of three layers (the sensory input layer, the hidden layer and the output layer), with 5, 3 and 1 neurons, respectively.

8.3. Support Vector Machines (SVMs). In the most cumbersome case, the patters are not linearly separable. The main objective of the SVM schemes is to map the input data from the N-dimensional space to the M-dimensional space (M>N), where the classes are supposed to be linearly separable and can be classified by the calculation of a standard separating hyperplane [64,65] (see Appendix S2 for details on the implementation of SVM).

In our work, polynomial and radial basis function (RBF) as well as linear SVM were used to classify the input data.

8.4. Normalization, Validation and Performance Measures. In order to train the classifiers and perform the KS-tests, all samples were normalized using the MinMax normalization [21].

There are several ways to compute the performance of a recognition system. The pattern recognition schemes were evaluated using two different procedures: The calculation of several performance measures such as sensitivity (Se), specificity (Sp), positive predictive value (Pp), negative predictive value (Np) and accuracy (Ac), all in the interval [0.00,100.00]. On the other hand, Receiver Operating Characteristic (ROC) curve was used in order to measure the accuracy of ANNs. The ROC curve is the plot of the true positive rate (Se) versus the false positive rate (1 − Sp) for different testing points in a diagnostic test. An ROC curve illustrates various aspects: First, it shows the tradeoff between the sensitivity and the specificity in the evaluation of a model; and second, it is a measure of the accuracy of the algorithm given by the area under the curve, i.e., the algorithm's probability of giving correct classifications when a new input pattern is presented [29].

9. Computational Implementation

For each subject statistical, spectral, multi-resolution and non-linear features were calculated using Matlab™ 7.6.0. The flow diagram of the whole system is depicted in Figure 2.

The application works with 5-min electrocardiographic (ECG) signals; thereby, a preprocessing step is involved in the procedure, i.e., the R-peak extraction and NN intervals calculation. Therefore, there is an ectopic beat removing algorithm, i.e., Grubbs Test extended by Rosner outlier detector. The next stage contains the feature extraction, i.e., statistical, spectral, multi-resolution and non-linear features calculation. For spectral features calculation, the 4 Hz cubic interpolation and the smoothness priors $\lambda=1000$ as detrending method are performed in the whole HRV dataset. The wavelet packet-based features are extracted using DB4 mother wavelet and the decomposition is done to a level $m=5$ [21]. Ellipse fitting and histogram features are extracted from the first-order Poincaré plot. SmEn and ApEn complexity measures are extracted using $r=0.1\sigma$ and $m=1:4$. All the features mentioned above can be displayed by the user. Feature selection is performed via KS-tests and the top-5 features are used to distinguish normal subjects (N) from cardiovascular risk ones (R). The classification scheme is responsible for giving the final prognosis result.

The respiratory rate mean and standard deviation feature can be used to corroborate that respiratory rate is relatively constant over the whole ECG record and that is approximately equal to 12 breaths/min. If this condition is not fulfilled, the results would be invalid.

Results

1. Statistical, Spectral, Multi-resolution and Non-linear Analysis of Extracted HRV Data

All the feature analysis results obtained in this work were reported using standard box diagrams, given their suitability for this statistical analysis and since their interpretation can be performed in a remarkably easy way, regardless of the fact that variables could present a great deviation from the normal distribution. The tops and bottoms of each box are the 25th and 75th percentiles of the samples, respectively. The line in the middle of each box is the sample median; this illustrates the skewness of the samples. The dashed lines extending below and above each box are drawn from the ends of the interquartile ranges to the furthest observation within the dashed line length. Crosses are the outliers of the samples; they represent atypical data sufficiently distant from the limits of the box. Note that their elimination is not justified, provided that the objective of box diagrams is to give a complete knowledge of the shape of the data distribution.

Statistical, spectral, multi-resolution and non-linear features were calculated from the recorded HRV database. The statistical analysis for the classical measures is shown in Figure 3.

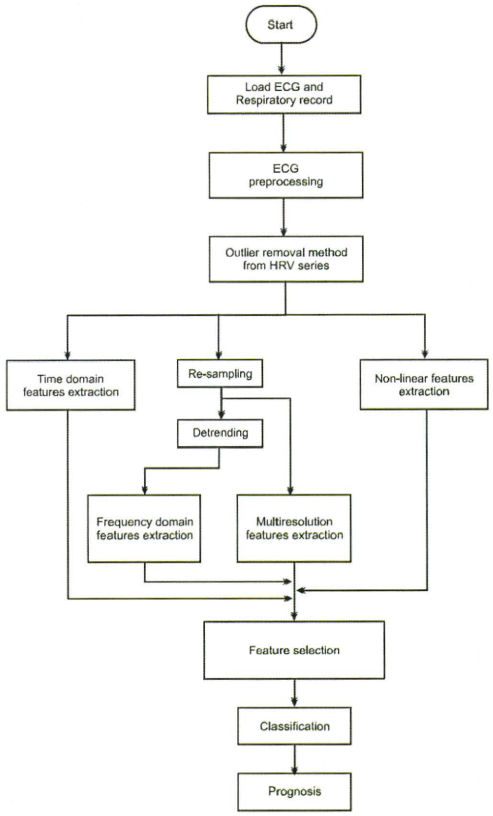

Figure 2. Flow diagram of the computational implementation of the computational tool reported in this work.
doi:10.1371/journal.pone.0017060.g002

The KS-test showed that all statistical features (mean, standard deviation, RMSSD, pNN50, MIRR, MDARR and SDSD) are statistically significant ($p<0.05$) for the comparison of normal (N) and cardiovascular risk (R) subjects. The most statistically significant features were the standard deviation, RMSSD, MIRR and SDSD (with $p<0.001$); the remaining features reported significances close to the alpha value.

In addition, LF power, LF/HF ratio, NLF power and NHF power showed statistically significant differences ($p<0.05$) between normal and cardiovascular risk subjects; however, VLF and HF powers do not discriminate between these two groups ($p>0.05$).

Standard PCA was applied to the multi-resolution measures in order to obtain the most relevant features in terms of variance. The total of selected groups of wavelet coefficients was 26 out of 62 (the total of wavelet packet coefficients from a decomposition level of 5). These 26 groups of coefficients, according to the PCA, retain approximately 98% of the variance of the model; however, the

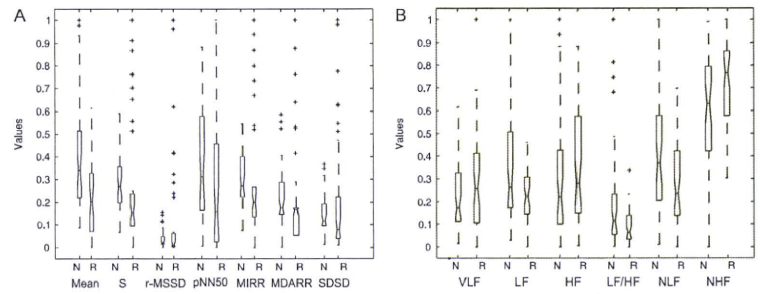

Figure 3. Box diagrams. (a) Statistical measures and, (b) Spectral measures from 5-min HRV records from normal (N) and risk (R) subjects in normalized values (*y* axis).
doi:10.1371/journal.pone.0017060.g003

features projections given by this transformation were not used to train the classifiers due to the decreasing statistical significance of the projected features. The main results of PCA for the two principal components are illustrated in Figure 4. The second principal component projection showed statistical significance in both energy and entropy wavelet features; these two features retain approximately 50% of the variance of the model. In this analysis, even the third component showed statistical significance; however, the rest of the projected data were not significantly different or discriminative between normal and cardiovascular risk subjects.

A total of 27 wavelet packet-based features were selected. Statistical significance levels of the entropy measures showed that 15 wavelet entropy components were statistically significant with $0.00001<p<0.05$ (1 from the first decomposition level, 2 from the second one, 1 from the third one, 3 form the fourth one and 8 from the last one). On the other hand, the significance levels for energy features showed that 12 wavelet energy components were statistically significant with $0.003<p<0.05$ (1 from the first decomposition level, 1 from the second one, 2 from the third one, 3 form the fourth one and 5 from the last one). The remaining entropy and energy components were not taken into account because they did not discriminate between the two groups (normal and cardiovascular risk subjects) with statistical significance.

Non-linear analysis KS-test results are illustrated in Figure 5. The results of the non-linear analysis showed that SD1 and SD2 ellipse fitting features are statistically significant ($p<0.01$, in the best case); SD1 being the less significant one. Additionally, there is statistical difference in histogram technique parameters, i.e., the widths of the NN intervals, the width and the length histograms of the HRV records, among normal and cardiovascular risk subjects. According to the statistical analysis, statistical significance increases with the NN intervals histogram width ($p<0.00001$) and the length histogram width ($p<0.00001$). For the case of the width of the width histogram the statistical difference is relatively high ($p<0.01$).

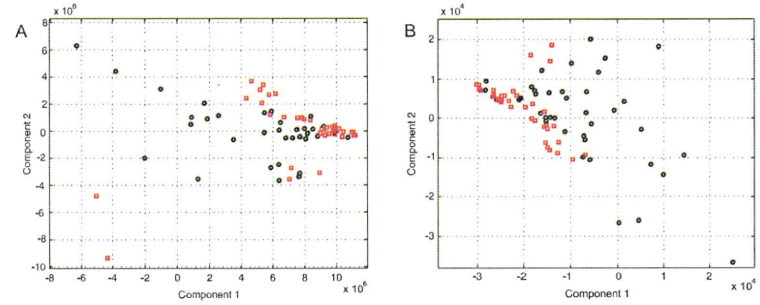

Figure 4. PCA transform of multi-resolution features of the 5-min HRV records from Normal (black diamond) and cardiovascular risk (red square) subjects. (a) entropy features and, (b) energy features.
doi:10.1371/journal.pone.0017060.g004

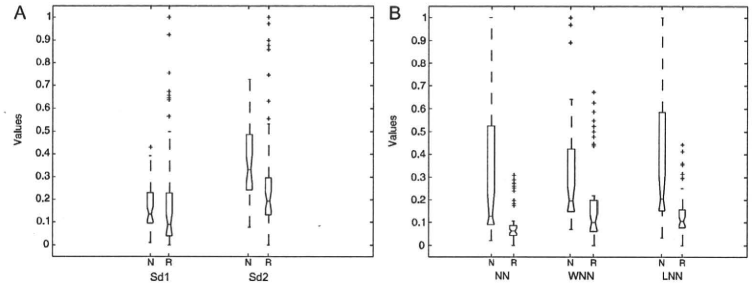

Figure 5. Box diagrams of Poincaré map-based features. (a) SD1 and SD2 ellipse fitting features and, (b) NN histogram (NN), width histogram (WNN) and length histogram (LNN) features of the 5-min HRV records from normal (N) and risk (R) subjects in normalized values (*y* axis).
doi:10.1371/journal.pone.0017060.g005

ApEn and SmEn significance test results are contained in Figure 6. ApEn shows increased statistical significance ($p<10^{-7}$) for $m=1:4$. On the other hand, SmEn shows statistical significance ($p<0.001$) only for $m=1:3$, for $m=4$ there is no statistical significance for the comparison of normal (N) and cardiovascular risk (R) subjects. Table 2 contains the p values of ApEn and SmEn at various m values; the m value varies from 1 to 4. The subsequent values did not allow obtaining statistically significant ApEn and SmEn values due to the relatively short duration of the HRV records (5-min per HRV record) [20].

The total number of features extracted from spatial and frequency domains, multi-resolution and non-linear algorithms is equal to 52 (7 statistical, 6 spectral, 27 multi-resolution and 12 non-linear features). The total number of optimal features extracted by KS-tests is equal to 5 due to the statistically significant discrimination presented by them (the next section will illustrate this fact clearly). The resulting feature set combined 3 non-linear and 2 multi-resolution features. These features were used to train and test the ANN and SVM classifiers. Additional experiments were conducted in order to compare the performance of the four principal PCA feature projections to those chosen by KS-tests.

2. Artificial Intelligence Schemes Classification for the Prognosis of Cardiovascular Risk

2.1. KS test-based Feature Selection Results. In order to evaluate each artificial intelligence (AI) scheme, the cross validation method was used. This method allows generating the indexes for the validation of the N observations by choosing randomly the training and test observations. Each AI scheme was trained using approximately 66% of the observations (60 HRV records, 30 from normal subjects and 30 from cardiovascular risk subjects) and tested using the remaining 33% of them (30 HRV records, 15 from normal subjects and 15 from cardiovascular risk

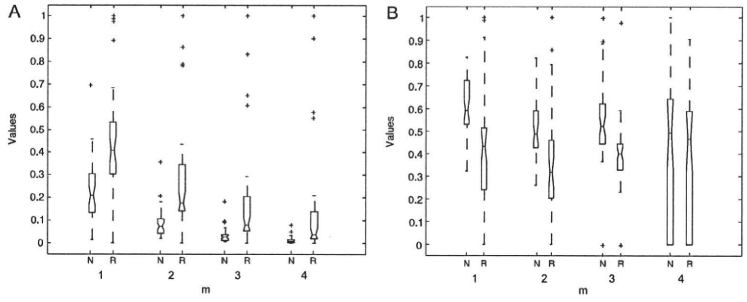

Figure 6. Box diagrams of complexity measures. (a) ApEn and, (b) SmEn ($r=0.1\sigma$ and $m=1-4$) of the 5-min HRV records from normal (N) and risk (R) subjects in normalized values (*y* axis).
doi:10.1371/journal.pone.0017060.g006

Table 2. Statistical significance for complexity measures at different m values.

m	p-value (ApEn)	p-value (SmEn)
1	1.87E-08	2.38E-07
2	1.21E-09	1.60E-04
3	4.87E-09	2.52E-06
4	6.83E-08	0.6101

doi:10.1371/journal.pone.0017060.t002

patients). This division gave an optimal performance (high generalization levels) for the ANNs as well as for SVMs.

Experiments were performed using 5 (3 from non-linear domain and 2 from multi-resolution domain), 10 (4 from non-linear domain, 3 from multi-resolution domain and 3 from statistical domain) and 15 features (5 from non-linear domain, 6 from multi-resolution domain and 4 from statistical domain) selected by KS-test. The results of MLP and RBF neural networks as well as of SVM classifications of HRV records from normal (N) and cardiovascular risk (R) subjects are illustrated in Table 3. The ROC curves for both neural network schemes are depicted in Figure 7; the areas under the curve are 0.9822, 0.8889 and 0.9024 for MLP; and 0.8800, 0.8667 and 0.8400 for RBFNN, for 5, 10 and 15 features, respectively. The linear SVM C value was fixed to 1 by default. The SVM with polynomial and RBF kernels' C and γ parameters produced the best classification performances. All $C\neq$ and γ were determined into a heuristic way.

According to Table 3, the higher performance was reached by MLP using the top-5 features selected by KS-test. It is important to note that the performance of the classifiers was similar in all cases; therefore, many combinations of features are suitable for the prognosis of cardiovascular risk as it is proposed in our work. For the 5 optimal features, linear SVM selected 36 support vectors;

Table 3. MLP, RBF neural networks and linear SVM ($C=1$), SVM with polynomial kernel ($C=1$; $\gamma=4$) and SVM with RBF kernel ($C=1$; $\gamma=3$) classifications using the top 5, top 10 and top 15 features selected via KS-test of the HRV records from normal (N) and cardiovascular risk (R) subjects.

#Features	Classifier		Se (%)	Sp (%)	Np (%)	Pp (%)	Ac (%)
5	MLP*	Training set	100.00	100.00	100.00	100.00	100.00
		Test set	93.33	100.00	93.75	100.00	96.67
	RBFNN*	Training set	96.67	100.00	96.67	100.00	98.33
		Test set	85.71	93.33	87.50	92.31	89.66
	SVM (Linear)	Training set	71.88	75.00	70.00	76.67	73.33
		Test set	72.73	72.73	72.73	72.73	72.73
	SVM (Polynomial kernel)	Training set	100.00	100.00	100.00	100.00	100.00
		Test set	84.09	70.45	81.58	74.00	80.00
	SVM (RBF kernel)	Training set	100.00	100.00	100.00	100.00	100.00
		Test set	74.24	78.79	75.36	77.78	76.52
10	MLP*	Training set	100.00	100.00	100.00	100.00	100.00
		Test set	86.67	80.00	85.71	81.25	83.33
	RBFNN	Training set	96.67	90.00	96.43	90.63	93.33
		Test set	60.00	100.00	71.43	100.00	80.00
	SVM (Linear)	Training set	100.00	100.00	100.00	100.00	100.00
		Test set	86.36	77.27	85.00	79.17	81.82
	SVM (Polynomial kernel)	Training set	100.00	100.00	100.00	100.00	100.00
		Test set	86.36	75.00	84.62	77.55	80.68
	SVM (RBF kernel)*	Training set	100.00	100.00	100.00	100.00	100.00
		Test set	96.97	81.82	96.43	84.21	89.39
15	MLP*	Training set	100.00	100.00	100.00	100.00	100.00
		Test set	73.33	100.00	78.95	100.00	86.67
	RBFNN	Training set	83.33	83.33	83.33	83.33	83.33
		Test set	60.00	100.00	72.43	100.00	80.00
	SVM (Linear)	Training set	100.00	100.00	100.00	100.00	100.00
		Test set	77.27	77.27	77.27	77.27	77.27
	SVM (Polynomial kernel)	Training set	100.00	100.00	100.00	100.00	100.00
		Test set	90.91	70.45	88.57	75.47	80.68
	SVM (RBF kernel)*	Training set	100.00	100.00	100.00	100.00	100.00
		Test set	93.94	77.27	92.73	80.52	85.61

*Classifiers that presented the higher performances on each experiment.
doi:10.1371/journal.pone.0017060.t003

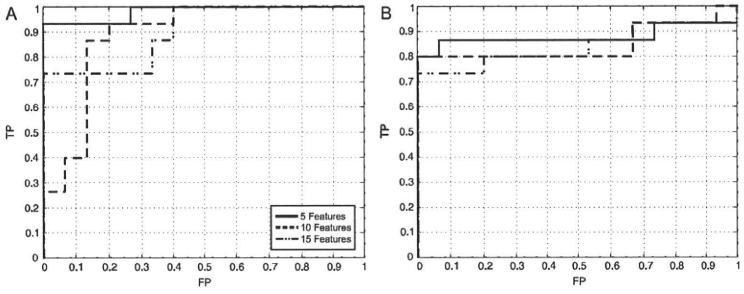

Figure 7. ROC curves. (a) For MLP neural networks, (b) RBF neural networks obtained from the classification of the HRV test records using 5, 10 and 15 top features selected by KS-test; the areas under the curves are equal to 0.9822, 08889 and 0.9024 for MLP and 0.8800, 0.8667 and 0.8400 for RBFNN, respectively.
doi:10.1371/journal.pone.0017060.g007

polynomial kernel SVM selected 28 support vectors; and RBF kernel SVM selected 43 support vectors from the same training dataset.

In addition, as part of the experiments, we evaluated the effect of using all the features from all the analysis methods shown in this paper. The results showed that for SVM classifiers, the three schemes evaluated (linear, polynomial kernel and RBF kernel SVM) reached higher performances than ANN ones. The main results of these experiments are registered in Table 4. The results of ANN classification were not included due to the poorness of the classification performances, this is a common effect given by the overfitting produced by the high dimensionality of the input space.

2.2. Do Multi-resolution and Non-linear Features Perform Better than Conventional Statistical and Spectral Features? A topic of remarkable discussion has been whether non-linear and multi-resolution features on HRV analysis perform better than the conventional and clinical-applied statistical and spectral analysis methods [2,27,28,29,30,31]. On the basis of determining the real usefulness of the non-linear and multi-resolution features in terms of the prognostic value (Se, Sp, Pp, Np and Ac), extensive experiments were carried out in this work.

Table 4. Results of linear SVM ($C=1$), SVM with polynomial kernel ($C=1$; $\gamma=4$) and SVM with RBF kernel ($C=1$; $\gamma=3$) classifications using the total of features of the HRV records from normal (N) and cardiovascular risk (R) subjects.

Kernel		Se (%)	Sp (%)	Np (%)	Pp (%)	Ac (%)
Linear	Training set	100.00	100.00	100.00	100.00	100.00
	Test set	86.36	90.91	86.96	90.48	88.64
Polynomial	Training set	100.00	100.00	100.00	100.00	100.00
	Test set	79.55	86.36	85.37	80.85	82.95
RBF	Training set	100.00	100.00	100.00	100.00	100.00
	Test set	77.27	87.88	86.44	79.45	82.58

doi:10.1371/journal.pone.0017060.t004

The proposed classifiers were trained using statistical and spectral features (classical analysis features) and using the multi-resolution and non-linear features (novel features) separately, especially in order to know the overall suitability of each group of features with respect to the HRV analysis. The main results of our experiments are depicted in Table 5. The ANN and SVM schemes were implemented under the same setup as described in the previous section. When statistical and spectral features were used to classify the data, the number of support vectors chosen by linear SVM, polynomial kernel SVM and RBF kernel SVM was 36, 24 and 46, respectively. On the other hand, when multi-resolution and non-linear features were used, linear SVM, polynomial kernel SVM and RBF kernel SVM selected 30, 24 and 46 support vectors, respectively.

Table 5 illustrates at least two important findings from the experiments carried out for this part of the research: First, non-linear and multi-resolution features have remarkably higher prognostic value than the features referred to as classical analysis (this fact was also confirmed by the statistical significance of the features already reported in this work); and second, the results indicate indirectly the overall usefulness of certain combinations of statistical and spectral measures and their expected effectiveness in clinical applications (it is important to note that even when these classical features are not very suitable to HRV analysis, the non-linear nature of the classifiers is the main catalyst to reach moderately good performances).

Due to the non-linearity and non-stationarity of the HRV signal, many authors prefer using non-linear and multi-resolution features rather than statistical or spectral ones in order to train classifiers [20,21]. Nonetheless, it is important to note that as the complexity of the features increases, also its medical interpretation becomes obscure and cumbersome. Furthermore, especially multi-resolution decomposition produces an important loss on the potential interpretation of features and signals, regardless of the remarkable increase of the statistical significance of the features reported using such analyses.

2.3. PCA-based Feature Selection Results. In addition to the results reported above, several classification experiments regarding PCA features' projections were performed in our work. They were carried out using the cross validation method

Table 5. MLP, RBF neural networks and linear SVM ($C=1$), SVM with polynomial kernel ($C=1$; $\gamma=4$) and SVM with RBF kernel ($C=1$; $\gamma=3$) classifications using classical and non-linear/multi-resolution features of the HRV records from normal (N) and cardiovascular risk (R) subjects.

Features	Classifier	Se (%)	Sp (%)	Np (%)	Pp (%)	Ac (%)
Statistical + Spectral	MLP	66.67	60.00	64.29	62.50	63.33
	RBFNN	26.67	93.33	56.00	80.00	60.00
	SVM (Linear)	72.73	86.36	76.00	84.21	79.55
	SVM (Polynomial kernel)	68.18	70.45	68.89	69.77	69.32
	SVM (RBF kernel)	68.18	74.24	70.00	72.58	71.21
Non-linear + Multi-resolution	MLP	80.00	100.00	83.33	100.00	90.00
	RBFNN	73.33	100.00	78.95	100.00	86.67
	SVM (Linear)	95.45	77.27	94.44	80.77	86.36
	SVM (Polynomial kernel)	88.64	81.82	87.80	82.98	85.23
	SVM (RBF kernel)	90.91	83.33	90.16	84.51	87.12

doi:10.1371/journal.pone.0017060.t005

under the same setup reported above. These experiments were made on the basis of two main goals: First, in order to investigate whether the significance levels of the projected features remained similar to the original ones; and second, to classify the data using the 3, 4, 5 and 10 principal features' projections from such PCA analysis, as the variance retained by the 3, 4, 5 and 10 first components for both groups –normal healthy subjects and cardiovascular risk patients– was equal to 77.65%, 83.33%, 86.96% and 94.45%, respectively. Furthermore, the 99% of the variance of the model was retained by the first 21 components. According to the KS-test results, from the five first PCA projections, three of them remained to be statistically significant ($p<0.03$), and in one case, the seventh PCA projection also showed high statistical significance ($p<0.04$); the rest of the components were not statistically significant for the comparison of normal (N) and cardiovascular risk (R) subjects.

The results of the ANN and SVM schemes classification of HRV records from normal (N) and cardiovascular risk (R) subjects are depicted in Table 6. With respect to the classification results using the projected features, linear SVM selected 46, 32, 27 and 23 support vectors from the whole training dataset; polynomial kernel SVM chose 28, 22, 21 and 21 support vectors; and RBF kernel SVM picked up 46 support vectors in all cases. Table 6 clearly illustrates important improvements for the performance of SVM-based classifiers. On the other hand, MLP and RBFNN schemes presented highly limited performances over the entire track of experiments regarding the implementation of PCA. However, the greatest performance reported by our work was achieved by MLP when the KS test-based feature selection was performed.

The main aim of using these four different numbers of PCA projections was to compare the performance reached by the classifiers and to identify whether the data structure was suitable for the proposed classifiers architecture. Indeed, there exists more than one group of features that reported high success rates at classifying the HRV records. Amongst all the classifiers, the maximum overall performance was reached by the polynomial kernel SVM with overall sensitivity, specificity and accuracy of 90.91%, 93.18% and 92.05%, respectively.

Discussion

Heart rate variability has been related to numerous cardiac diseases. According to the literature, the short variations on statistical features of the NN intervals are related to: Complete heart block (CHB), left bundle branch block (LBBB) and ischemic cardiopaty. On the other hand, the long variations on statistical features of the NN intervals are related to: Premature ventricular contractions (PVCs), sinus syndrome (SSS) and atrial fibrillation (AF). There are several modifications on AR spectrums that can be noticed by the calculation of the power in frequency bands. Short variations of HRV segments usually lead to high VLF and LF bands power. Conversely, long variations of HRV segments, usually leads to higher HF band power. As cardiovascular risk is highly related to variations on statistical and spectral components, one of the major disadvantages of these methods is the linearity and consequently, their poor suitability for highly non-stationary HRV dynamics and, certainly, the NN intervals fluctuation by nervous mechanisms. The Fourier transform techniques (frequency domain methods such as Welch periodogram or AR spectrum as well) resolve the time domain signal into complex exponential functions, along with information about their phase shift measured with respect to a specific reference instant. Here the frequency components extend from $-\infty$ to ∞ in the time scale. That is, even finite length signals are expressed as the sum of frequency components of infinite duration. Besides, the phase angle, being a modular measure, fails to provide the exact location of an 'event' along the time scale. This is a major limitation of the Fourier transform approach [2]. Thereby, considering the cardiovascular system as nonlinear in nature, can lead to a better understanding of its dynamics.

The patterns in HRV are directly related to the Poincaré map patterns in visual assessment. In the case of short fluctuations, HRV segments are not much dispersed and torpedo shapes [62] are predominant in many cases. In the case of long fluctuations, HRV segments appear to be very dispersed forming complex-like and fan-like return map shapes. All these Poincaré plot patterns are directly related with cardiovascular risk [66].

One of the main contributions of this work is the prognosis of cardiovascular risk in a general way, not only for specific cardiac diseases or the prediction of specific cardiac episodes like other publications have shown [1,8,13,14,16,18,19,20,21,29,55,61]. Moreover, it has been confirmed that multi-resolution and non-linear analysis are much more suitable for the assessment and prognosis of cardiovascular risk than statistical and spectral classical analysis. KS significance tests also confirmed that those features lead to higher statistical significance levels ($p<0.001$ for

Table 6. MLP, RBF neural networks and linear SVM ($C=1$), SVM with polynomial kernel ($C=1$; $\gamma=4$) and SVM with RBF kernel ($C=1$; $\gamma=3$) classifications using the projections of the features from PCA analysis of the HRV records from normal (N) and cardiovascular risk (R) subjects.

Number of PCA Projections	Classifier	Se (%)	Sp (%)	Np (%)	Pp (%)	Ac (%)
3	MLP	60.00	73.33	64.71	69.23	66.67
	RBFNN	40.00	93.33	60.87	85.71	66.67
	SVM (Linear)	77.27	63.64	73.68	68.00	70.45
	SVM (Polynomial kernel)	84.09	70.45	81.58	74.00	77.27
	SVM (RBF kernel)	89.39	65.15	86.00	71.95	77.27
4	MLP	80.00	80.00	80.00	80.00	80.00
	RBFNN	46.67	86.67	61.90	77.78	66.67
	SVM (Linear)	90.91	90.91	90.91	90.91	90.91
	SVM (Polynomial kernel)	90.91	93.18	91.11	93.02	92.05
	SVM (RBF kernel)	93.94	89.39	93.65	89.86	91.67
5	MLP	66.67	100.00	75.00	100.00	83.33
	RBFNN*	N/A	N/A	N/A	N/A	N/A
	SVM (Linear)	86.36	95.45	87.50	95.00	90.91
	SVM (Polynomial kernel)	81.82	95.45	84.00	94.74	88.64
	SVM (RBF kernel)	81.82	95.45	84.00	94.74	88.64
10	MLP	80.00	73.33	78.57	75.00	76.67
	RBFNN*	N/A	N/A	N/A	N/A	N/A
	SVM (Linear)	81.82	81.82	81.82	81.82	81.82
	SVM (Polynomial kernel)	81.82	95.45	84.00	94.74	88.64
	SVM (RBF kernel)	81.82	95.45	84.00	94.74	88.64

*The results for this classifier were not reported due to their poorness.

doi:10.1371/journal.pone.0017060.t006

the case of ApEn and SmEn features). We developed a method that combines statistical, spectral, multi-resolution and non-linear features as well as ANN and SVM schemes for the prognosis of cardiovascular risk. Exactly 90 HRV records were analyzed, 60 of them were used to train and 30 to test each classification scheme.

From the classification schemes, MLP provided the best classification rates for the prognosis of cardiovascular risk, with an area under the ROC curve equal to 0.9800. On the other hand, schemes such as the RBF network and SVMs showed relatively high classification performances too. Another remarkable finding is the improvement of the classification rates of SVM using all the extracted features (not only the features selected by KS significance tests) and PCA, which can be attributable to the computation of the decision surface and the apparent SVM bias towards the positive and negative cases. Furthermore, as expected, ANN schemes often presented overfitting using all those features. The comparison between the performances of all the implemented classifiers was limited to sensitivity, specificity, positive predictive value, negative predictive value and accuracy as a consequence of ROC curves limitations, i.e., usually its contributions become cumbersome when a comparison between different classifiers is needed. Besides, their transformation to objective values is usually limited to the calculation of the area under the curve [67].

According to findings reported in the literature [5], breath rate modifies the fluctuation of the NN intervals in a HRV sample record, i.e., there is an evident modification of the HRV when the analyzed subject is breathing at different frequencies (e.g., 6 breaths/min or 12 breaths/min) provided that the rhythmic fluctuations can be larger or shorter given the regulation mechanisms and the RSA dynamics as an effect of the activity of neural oscillators. As a direct consequence, the experimental results from the comparison between records at different breathing rates would be invalid. Thus, another contribution of this work is the consideration of the breathing rate as an additional variable for the assessment of HRV; this feature was included in every record taken for the HRV database reported in this work.

Besides the strong considerations of the breathing rate and the breathing signal, our computational implementation allows working with the ECG and HRV signals for medical analysis. There are new possibilities of analysis that commercial and conventional HRV analysis software [55] have not yet considered; additionally, there is the possibility of performing an automatic prognosis using a trained ANN scheme embedded in the program. The main objective of this module is to give support to the specialist criteria on the HRV assessment. This computational application needs strong validation and medical feedback, which will be a topic for future research.

According to the results of this study, we strongly suggest working with multi-resolution and non-linear analysis in order to achieve more reliable cardiovascular risk prognosis, especially for classification schemes such as ANNs and SVMs. It is evident that a nonlinear deterministic approach is more appropriate to describe more complex phenomena, indicating that apparently erratic behavior can be generated even by a simple deterministic system with nonlinear structure. In general terms, the fluctuations of heartbeats during normal sinus rhythm could be partially attributed to deterministic chaos, and a decrease in this type of nonlinear variability could be observed in different cardiovascular diseases [58]. Further investigation is needed for the incorporation of chaotic dynamics and fractals to the analysis of HRV for the prognosis of cardiovascular risk proposed in this study.

Conclusions

This work has been focused on 4 major aspects: (1) The HRV database conformation integrating the breathing signal; (2) integrating the breathing frequency to the analysis of HRV records; (3) the analysis of statistical, spectral, multi-resolution and non-linear features linked with classification schemes for the prognosis of cardiovascular risk as well as the confirmation of the properties of these features as they are reported in the literature; (4) a brief illustration of the software implementation of advanced HRV analysis integrating an automatic prognosis tool using a standard 5 min ECG record.

This work has developed a method for the cardiovascular risk prognosis using statistical, spectral, multi-resolution and non-linear features extracted from HRV data. The database used in this work was recorded using a proper medical protocol and contains a total of 90 HRV and breathing signal records from normal and cardiovascular risk subjects. The suitability of each HRV analysis feature has been shown by using KS-tests and neural and support vector classifiers. Short-term HRV features are highly useful for the prognosis of cardiovascular risk; nonetheless, long-term features can be useful for increasing the positive predictive value of the proposed classifiers.

In addition, it has become obvious that the performance reported by the different feature selection strategies depends largely on the pattern recognition scheme implemented to classify the data. For the short-term HRV features analyzed in this work, there were two main observed effects: First, the ANN schemes were more suitable for the KS test-based feature selection as well as for feature spaces of low dimension; and second, SVM schemes were more suitable for the PCA-based feature selection as well as to high dimensional feature spaces. Nonetheless, as the PCA projected features improved by far the performance of SVM classifiers, their statistical significance showed influential decrease that affected negatively the performance of the ANN classifiers.

Breathing signal and breathing frequency were employed in this work for the analysis of HRV, given the findings about RSA phenomena on the modification of the fluctuations of NN intervals at different breathing frequencies [5]. All the HRV measurements in this work were done approximately at 12 breaths/min for every single subject in the database; this was guaranteed by the procedures established in the medical protocol that we designed to carry out this research; moreover, the acquired breathing signals confirmed it.

Finally, HRV signal –as both a traditional and non-linear signal in nature– has been an important predictor of cardiovascular risk. Furthermore, this work represents an important step in comprehensively understanding such dynamics, and more importantly, on the prognosis of cardiovascular risk as a stated goal established by Chattipakorn et al. (2007) and a plethora of researchers and clinicians: "It is necessary to understand the mechanisms of HRV components and improve their sensitivity and specificity as a prognostic marker" [68]. Furthermore, the combination of the methods reported in this work and other ECG and physiological parameters is expected to lead to a solution for the prognosis of cardiovascular mortality at reasonable cost-effectiveness.

Supporting Information

Appendix S1 Detailed description of complexity measures calculation.
(DOC)

Appendix S2 Detailed description of SVM learning algorithm.
(DOC)

Acknowledgments

We acknowledge the support of the Occupational Health Office (Universidad Autonoma de Occidente), the Coomeva IPS S. A. experts and the patients which formed part of this study. We also acknowledge the special reviewing collaboration of Dr. Odelia Schwartz (Albert Einstein College of Medicine, NY, USA). Finally, we are grateful for the important suggestions given by anonymous reviewers.

Author Contributions

Conceived and designed the experiments: JFR ELE. Performed the experiments: JFR ELE PCE WAR. Analyzed the data: JFR ELE. Contributed reagents/materials/analysis tools: DFR. Wrote the paper: JFR DFR. Performed the feature extraction methods: JRV. Gave important feedback on statistical procedures: ELE. Made the PCA-based feature selection and classification experiments: JRV. Gave important feedback and medical validation of the reported results: WAR. Gave important scientific background: DFR. Suggested suitable classification schemes and architectures to overcome the classification problems: DFR. Gave important feedback for the enhancement of the paper: DFR PCE.

References

1. Mohammadzadeh Asl B, Kamaledin Setarehdan S, Mohebbi M (2008) Support vector machine-based arrhythmia classification using reduced features of heart rate variability signal. Artificial Intelligence in Medicine 44: 51–64.
2. Rajendra Acharya U, Paul Joseph K, Kannathal N, Min Lim C, Suri JS (2006) Heart rate variability: a review. Med Bio Eng Comput 44: 1031–1051.
3. Bezerianos A, Papadimitriou S, Alexopoulos D (1999) Radial basis function neural networks for the characterization of heart rate variability dynamics. Artificial Intelligence in Medicine 15: 215–234.
4. Belova NY, Mihaylov SV, Piryova BG (2007) Wavelet transform: A better approach for the evalation of instantaneous changes in heart rate variability. Autonomic Neuroscience: Basic and Clinical 131: 107–122.
5. Lopes P, White J (2006) Heart rate variability: Measurement methods and practical implications. In: Maud PJ, Foster C, eds. Physiological Assessment of Human Fitness. pp 39–61.
6. García-González MA (1998) Estudio de la Variabilidad del ritmo cardiaco mediante técnicas estadísticas, espectrales y no-lineales. PhD Thesis, Universitat Politècnica De Catalunya.
7. Montano N, Porta A, Cogliati C, Costantino G, Tobaldini E, et al. (2008) Heart rate variability explored in the frequency domain: A tool to investigate the link between heart and behavior. Neuroscience and Biobehavioral Reviews. In Press.
8. Acharyaa UR, Bhatb PS, Iyengarc SS, Raod A, Dua S (2003) Classification of heart rate data using artificial neural network and fuzzy equivalence relation. Pattern Recognition 36: 61–68.
9. Kuss O, Schumann B, Kluttig A, Greiser KH, Haerting J (2008) Time domain parameters can be estimated with less statistical error than frequency domain parameters in the analysis of heart rate variability. Journal of Electrocardiology 41: 287–291.
10. Urbanowicza K, Zebrowski J, Baranowskic JR, Holyst JA (2007) How random is your heart beat?. Physica A 384: 439–447.
11. Bilgin S, Çolak OH, Koklukaya E, Ari N (2008) Efficient solution for frequency band decomposition problem using wavelet packet in HRV. Digital Signal Processing 18: 892–899.
12. Task force of the European society of cardiology and the North American society of pacing and electrophysiology (1996) Heart Rate Variability Standards of Measurement, Physiological Interpretation, and Clinical Use. Circulation 93: 1043–1065.
13. D'Addio G, Acanfora D, Pinna GD, Maestri R, Furgi G, et al. (1998) Reproducibility of Short -and Long-Term Poincaré Plot Parameters Compared with Frequency-Domain HRV Indexes in Congestive Heart Failure. Computers in Cardiology 25: 381–384.

14. D'Addio G, Pinna GD, Maestri R, Acanfora D, Picone C, et al. (1999) Correlation Between Power-law Behavior and Poincaré Plots of Heart Rate Variability in Congestive Heart Failure Patients. Computers in Cardiology 26: 611–614.
15. Thong T (2007) Geometric Measures of Poincaré Plots for the Detection of Small Sympathovagal Shift. Proceedings of the 29th Annual International Conference of the IEEE EMBS Cité Internationale. pp 4641–4644.
16. Woo MA, Stevenson WG, Moser DK, Trelease RB, Harper RM (1992) Patterns of beat-to-beat heart rate variability in advanced heart failure. Am Heart J 123: 704–710.
17. Brennan M, Palaniswami M, Kamen P (2001) Do existing measures of Poincare plot geometry reflect nonlinear features of heart rate variability?. IEEE Trans Biomed Eng 48: 1342–1347.
18. Rueda OL, López EJ, Vargas CA, Delgado MB, Murillo CA (2007) La variabilidad de la frecuencia cardiaca como factor pronóstico de mortalidad del infarto del miocardio: Revisión sistemática de estudios observacionales. Médica Sanitas 22.
19. Malik M, Farrell T, Cripps TR, Camm AJ (1989) Heart rate variability in relation to prognosis after myocardial infarction: selection of optimal processing techniques. Eur Heart J 10: 1060–1074.
20. Chesnokov YV (2008) Complexity and spectral análisis of the heart rate variability dynamics for distant prediction of paroxysmal atrial fibrillation with artificial intelligence methods. Artificial Intelligence in Medicine 43: 151–165.
21. Isler Y, Kuntalp M (2007) Combining classical HRV indexes with wavelet entropy measures improves to performance in diagnosing congestive heart failure. Computers in Biology and Medicine 37: 1502–1510.
22. Wolf MM, Varigos GA, Hunt D, Sloman JG (1978) Sinus arrhythmia in acute myocardial infarction. Med J Aust. pp 52–53.
23. Penaz J, Roukenz J, Van Der Waal HJ (1968) Spectral Analysis of Some Spontaneous Rhythms in the Circulation.. Leipzig Germany: Biokybernetik, Karl Marx University. pp 223–241.
24. Pomeranz M, Macaulay R, Caudill M, Ma K, Kutz I, et al. (1985) Assessment of autonomic function in humans by heart rate spectral analysis. Am J Physiol 248: H151–H153.
25. Akselrod S, Gordon D, Ubel FA, Shannon DC, Barger AC, et al. (1981) Power spectrum analysis of heart rate fluctuation: a quantitative probe of beat to beat cardiovascular control. Science. pp 220–222.
26. Akselrod S, Lishner M, Oz O, Bernheim J, Ravid M (1987) Spectral analysis of fluctuations in heart rate: an objective evaluation of autonomic nervous control in chronic renal failure. Nephron 45: 202–206.
27. Berntson GG, Bigger JT, Jr., Eckberg DL, Grossman P, Kaufmann PG, et al. (1997) Heart rate variability: Origins, methods, and interpretive caveats. Psychophysiol 34: 623–648.
28. Broadman A, Schlindwein FS, Rocha AP, Leite A (2002) A study on the opimum order of autoregressive models for heart rate variability. Physiol Meas 23: 324–336.
29. Pagani M, Lombardi F, Guzzetti S, Rimoldi O, Furlan R, et al. (1986) Power spectral analysis of heart rate and arterial pressure variabilities as a marker of sympathovagal interaction in man and conscious dog. Circ Res 59: 178–193.
30. Pal GK, Pal P, Nanda N, Amudharaj D, Karthik S (2009) Spectral analysis of heart rate variability (HRV) may predict the future development of essential hypertension. Medical Hypotheses 72: 183–185.
31. Ravichandran IT, Ramasubba Reddy L Arudainayagam A (2003) Estimation and Power Spectral Analysis of Heart Instantaneous Frequency (HIF) - A Wavelet Approach. Bio-Signal Processing TENCON. pp 223–226.
32. Fukuda O, Nagata Y, Homma K, Tsuji T (2001) Evaluation of heart rate variability by using wavelet transform and a recurrent neural network. Proceedings of the 23rd Annual EMBS International Conference. pp 1769–1772.
33. Lerma C, Infante O, Perez-Grovas H, Jose MV (2003) Poincaré plot indexes of heart rate variability capture dynamic adaptations after haemodialysis in chronic renal failure patients. Clin Physiol & Func Im 23: 72–80.
34. Marciano F, Migaux ML, Acanfora D, Furgi G, Rengtif F (1994) Quantification of Poincaré Maps for the Evaluation of Heart Rate Variability. Computers in Cardiology. pp 577–580.
35. Singh D, Vinod K (2005) Effect of RR Segment Duration on Short-Term HRV Assessment Using Poincaré Plot. Proceedings of ICISIP. pp 430–434.
36. Brennan M, Palaniswami M, Kamen P (2002) Poincaré plot interpretation using a physiological model of HRV based on a network of oscillators. Am J Physiol Heart Circ Physiol 283: 1873–1886.
37. Hnatkova K, Copie X, Staunton A, Malik M (1995) Numeric processing of Lorenz plots of R–R intervals from long-term ECGs. Comparison with time-domain measures of heart rate variability for risk stratification after myocardial infarction. J Electrocardiol 28: 74–80.
38. Wolf A, Swift JB, Swinney HL, Vastano JA (1985) Determining Lyapunov exponents from a time series. Physica 16D: 285–317.
39. Kobayashi M, Musha T (1982) 1/f fluctuation of heartbeat period. IEEE Trans Biomed Eng 29: 456–257.
40. Goldberger AL (1996) Non-linear dynamics for clinicians: chaos theory, fractals, and complexity at the bedside. Lancet 347: 1312–1314.
41. Peng CK, Havlin S, Hausdorf JM, Mietus JE, Stanley HE, et al. (1995) Fractal mechanisms and heart rate dynamics. Long-range correlations and their breakdown with disease. J Electrocardiol 28: 59–65.
42. Hirsh JA, Bishop B (1981) Respiratory sinus arrhythmia in humans: how breathing pattern modulates heart rate. Am J Physiol Heart Circ Physiol 241: H620–H629.
43. Piepoli M, Sleight P, Leuzzi S, Valle F, Spadacini G, et al. (1997) Origin of Respiratory Sinus Arrhythmia in Conscious Humans. Circulation 95: 1813–1821.
44. Katona PG, Jih F (1975) Respiratory sinus arrhythmia: noninvasive measure of parasympathetic cardiac control. J Appl Physiol 39: 801–805.
45. Lloyd-Jones D, Adams R, Carnethon M, de Simone G, Ferguson TB, et al. (2009) Heart disease and stroke statistics – 2009 update: A report from the American Heart Association Statistics Committee and Stroke Statistics Subcommittee. Circulation 119: e21–e181.
46. Beltrán-Bohórquez JR (2010) Guías colombianas de cardiología. Síndrome coronario agudo con elevación del ST. Revista Colombiana de Cardiología 17: 111–275.
47. Gallagher D, Terenzi T, de Meersman R (1992) Heart rate variability in smokers, sedentary and aerobically fit individuals. Clinical Autonomic Research 2: 383–387.
48. Liao D, Carnethon M, Evans GW, Cascio WE, Heiss G (2002) Lower heart rate variability is associated with the development of coronary heart disease in individuals with diabetes: the atherosclerosis risk in communities (ARIC) study. Diabetes 51: 3524–3531.
49. Williams JS, Brown SM, Conlin PR (2009) Blood-pressure Measurement. N Engl J Med 360: e6.
50. Medvida SJ, Hurwitz BE, Lagreca AM, Llabre MM, Marks JB, et al. (1999) Aberrant parasympathetic and Hemodynamic function distinguishes a subgroup of psyrological distressed individuals with asymptomatic type-I diabetes mellitus, International Journal of Behavioral Medicine 6: 78–94.
51. Gutierrez A, Lara M, Hernandez PR (2005) Evaluación de un detector de complejo QRS basado en la wavelet de Haar usando las bases de datos MIT-BIH de arritmias y Europea del segmento ST y de la onda T. Computación y Sistemas 8: 293–302.
52. Lippman N, Stein KM, Lerman BB (1994) Comparison of methods for removal of ectopy in measurement of heart rate variability. Am J Physiol Heart Circ Physiol 267: H411–H418.
53. Rosner B (1983) Percentage Points for a Generalized ESD Many-Outlier Procedure. Technometrics 25: 165–172.
54. Ramirez-Villegas JF, Lam-Espinosa E (2009) Análisis de la variabilidad de la frecuencia cardiaca integrando la señal de la frecuencia respiratoria. B. Eng. Thesis, Universidad Autonoma de Occidente, Cali, Colombia.
55. Niskanen JP, Tarvainen MP, Ranta-Aho PO, Karjalainen PA (2002) Software for advanced HRV analysis. Computer Methods and Programs in Biomedicine. In Press.
56. Rosso OA, Blanco S, Yordanova J, Kolev V, Figliola A, et al. (2001) Wavelet entropy: a new tool for analysis of short duration brain electrical signals. J Neurosci Methods 105: 65–75.
57. Blanco S, Figliola A, Quian QR, Rosso OA, Serrano E (1998) Time-Frequency analysis of electroencephalogram series (iii): Information transfer function and wavelet packets. Phys Rev E 57: 932–940.
58. Lombardi F (2000) Chaos Theory, Heart Rate Variability, and Arrhythmic Mortality. Circulation 101: 8–10.
59. Meiss JD (2007) Differential dynamical systems. Society for Industrial and Applied Mathematics (SIAM). 434 p.
60. Sano M, Sawada Y (1985) Measurement of the Lyapunov spectrum from a chaotic time series. Physical Review Letters 55: 1082–1085.
61. Korpelainen JT, Sotaniemi KA, Mäkikallio A, Huikuri HV, Myllylä VV (1999) Dynamic Behavior of Heart Rate in Ischemic Stroke. Stroke 30: 1068–1073.
62. Pincus SM (2001) Assessing Serial Irregularity and its Implications for Health. Annals of the New York Academy of Sciences 954: 245–267.
63. Rencher AC (2002) Methods of Multivariate Analysis. Wiley Series in Probability and Statistics. 738 p.
64. Haykin S (1999) Neural Networks: A Comprehensive Foundation. Prentice Hall, inc. 823 p.
65. Wang L, Liu B, Wan C (2005) Classification using support vector machines with graded resolution. Proceedings of the international conference on granular computing. pp 666–670.
66. Woo MA, Stevenson WG, Moser DK, Trelease RB, Harper RM (1992) Patterns of beat-to-beat heart rate variability in advanced heart failure. Am Heart J 123: 704–710.
67. Fawcett T (2006) An introduction to ROC analysis. Pat Rec Leu 27: 861–874.
68. Chattipakorn N, Incharoen T, Kanlop N, Chattipakorn S (2007) Heart rate variability in myocardial infarction and heart failure. International Journal of Cardiology 120: 289–296.

Key Symposium

Journal of INTERNAL MEDICINE

doi: 10.1111/j.1365-2796.2010.02321.x

The pulse of inflammation: heart rate variability, the cholinergic anti-inflammatory pathway and implications for therapy

J. M. Huston[1] & K. J. Tracey[2]

[1]Department of Surgery, Division of General Surgery, Trauma, Surgical Critical Care, and Burns, Stony Brook University Medical Center, Stony Brook; and [2]Laboratory of Biomedical Science, The Feinstein Institute for Medical Research, Manhasset; NY, USA

Abstract. Huston JM, Tracey KJ (Department of Surgery, Division of General Surgery, Trauma, Surgical Critical Care, and Burns, Stony Brook University Medical Center, Health Sciences Center, Stony Brook; and Laboratory of Biomedical Science, The Feinstein Institute for Medical Research, Manhasset; NY, USA). The pulse of inflammation: heart rate variability, the cholinergic anti-inflammatory pathway, and implications for therapy (Key Symposium). *J Intern Med* 2011; **269**: 45–53.

Biological therapeutics targeting TNF, IL-1 and IL-6 are widely used for treatment of rheumatoid arthritis, inflammatory bowel disease and a growing list of other syndromes, often with remarkable success. Now advances in neuroscience have collided with this therapeutic approach, perhaps rendering possible the development of nerve stimulators to inhibit cytokines. Action potentials transmitted in the vagus nerve culminate in the release of acetylcholine that blocks cytokine production by cells expressing acetylcholine receptors. The molecular mechanism of this cholinergic anti-inflammatory pathway is attributable to signal transduction by the nicotinic alpha 7 acetylcholine receptor subunit, a regulator of the intracellular signals that control cytokine transcription and translation. Favourable preclinical data support the possibility that nerve stimulators may be added to the future therapeutic armamentarium, possibly replacing some drugs to inhibit cytokines.

Keywords: heart rate variability, inflammation, neuroimmunology, therapeutics, vagus nerve stimulation.

Introduction

Amongst the leading causes of morbidity and mortality in Western societies are heart disease, cancer, stroke, diabetes and sepsis. Recent advances in immunology reveal a significant pathogenic role for inflammation in the development and progression of these disorders. Inflammation accelerates deposition of atherosclerotic plaques leading to myocardial and cerebral infarction; mediates insulin resistance; stimulates tumour growth; and causes organ damage in lethal sepsis. Knowledge of these mechanisms has elevated the importance of understanding both the molecular basis of inflammation and the regulatory systems that keep it in check during health.

Inflammation is induced by factors that are exogenous (e.g. pathogens and microbial products) and endogenous [e.g. High Mobility Group Box-1 (HMGB1) released from injured cells] to the host [1, 2]. These inducing agents interact with genome encoded pattern recognition receptors expressed on monocytes, macrophages and other cells of the innate immune system [3]. These receptor families, including the toll-like receptors and NOD-like receptors, transduce intracellular signals leading to the production and release of cytokines, eicosanoids and other inflammatory molecules that directly mediate cellular responses causing inflammation [3]. The cardinal signs of inflammation, including pain, erythema, oedema, warmth and loss of function, can be produced by exposing tissues to inflammatory cytokines. Nonresolving or persisting exposure to cytokine damages tissue, impairs organ function and can be lethal. Biological therapeutics that specifically inhibit cytokine mediators of inflammation are widely used to treat arthritis, colitis, psoriasis and a growing list of other disabling illnesses. Therefore, the dangers of uncontrolled inflammation are inherent to the molecular activity of cytokines themselves, and maintenance of health requires tight control over the steps leading to the production and release of cytokines.

Factors that trigger inflammation also enhance the activity of anti-inflammatory pathways, which function to counter-balance inflammation. This concurrent activation of pro- and anti-inflammatory mechanisms is analogous to other homoeostatic systems, such as coagulation and fibrinolysis, which act in concert to coordinate haemostasis during haemorrhage. Anti-inflammatory pathways that exert critical roles in suppressing cytokine production include the hypothalamic-pituitary-adrenal axis, which culminates in glucocorticoid release; release of neutralizing soluble cytokine receptors; and production of anti-inflammatory cytokines (e.g. IL-10 and TGFβ). Interruption of these pathways (e.g. adrenalectomy), or failure of their function (genetic deficiency of IL-10) leads to excessive inflammation. This knowledge has enabled the development of novel therapies that suppress inflammation in humans by either directly targeting the activities of cytokines (e.g. anti-TNF antibodies), or by preventing cytokine release (glucocorticoids).

The inflammatory reflex suppresses inflammation

In the late 1990's, whilst studying CNI-1493, an inhibitor of the p38 MAP kinase developed by one of us (KJT) as an anti-inflammatory molecule, we discovered an anti-inflammatory neural circuit [4, 5]. Termed 'the inflammatory reflex', this neurological mechanism involves the vagus nerve, which can sense peripheral inflammation and transmit action potentials from the periphery to the brain stem [6]. This in turn leads to the generation of action potentials in the descending vagus nerve that are relayed to the spleen, where pro-inflammatory cytokine production is inhibited [7]. The molecular basis of this anti-inflammatory circuit, termed the cholinergic anti-inflammatory pathway, includes the neurotransmitter acetylcholine interacting with the alpha-7 nicotinic acetylcholine receptor subunit expressed on monocytes, macrophages and other cytokine producing cells [8]. Signal transduction through this receptor inhibits cytokine release, suppresses inflammation and confers protection against tissue damage in polymicrobial sepsis, arthritis, colitis, diabetes, atherosclerosis, ischaemia-reperfusion injury, pancreatitis, myocardial ischaemia and haemorrhagic shock [5, 9–20].

To date, the inflammatory reflex is the best- studied anti-inflammatory neural circuit, but undoubtedly, as expertise in this field continues to improve, it is likely that other pathways will be elucidated [21]. These findings now raise some fundamental questions about understanding clinical disease pathogenesis. Pre-eminent amongst these is whether it is possible to measure activity within the inflammatory reflex in humans in order to understand or predict the risk of uncontrolled inflammation. Here, we review available data addressing this question and focus on the potentially informative data regarding measurements of vagus nerve signalling. We discuss the concept that measuring changes in vagus nerve activity may provide useful information about real-time activity of the inflammatory reflex in patients with inflammatory diseases. We also examine the evidence that measuring underlying vagus nerve activity may have clinical utility for predicting damage from ongoing inflammation and review the potential implications of utilizing this diagnostic information to then guide therapeutic modulation of immune responses.

The cholinergic anti-inflammatory pathway

The 'cholinergic anti-inflammatory pathway' is the descending, or motor arc of the inflammatory reflex (Fig. 1) [6]. It is comprised of vagus nerve signals leading to acetylcholine- dependent interaction with the alpha 7 nicotinic acetylcholine receptor subunit (α7nAChR) on monocytes and macrophages, resulting in reduced cytokine production [8, 22]. The cholinergic anti-inflammatory pathway can be activated experimentally by electrical or mechanical vagus nerve stimulation, or through administration of α7 agonists, to inhibit inflammatory cytokine production, prevent tissue injury and improve survival in multiple experimental models of systemic inflammation and sepsis [4, 5, 9–14, 16–18]. Mononuclear cells express muscarinic and nicotinic acetylcholine receptors on their cell surface and experimental evidence suggests that α7 is required for the regulation of cytokine release by acetylcholine [8]. This pathway is unique in the context of vagus nerve signalling because in contrast to classical parasympathetic nervous system signalling through muscarinic receptors on target organs, this circuit requires signalling through a specific nicotinic receptor subunit.

Under basal conditions, the cholinergic anti-inflammatory pathway exerts a tonic, inhibitory influence on innate immune responses to infection and tissue injury. Interrupting this pathway, by either severing the vagus nerves, or by knocking out the α7 gene (*CHRNA7*), produces an inflammatory phenotype characterized by exaggerated responses to bacterial products and injury [5, 8]. For example, electrical stimulation of the cervical vagus nerve in wild-type

mice reduces pro-inflammatory cytokine production, but α7nAChR-knockout animals are resistant to these effects and produce higher levels of cytokines despite vagus nerve stimulation. Even in the absence of vagus nerve stimulation, α7nAChR-knockout mice generate a significantly elevated pro-inflammatory cytokine response following challenge with endotoxin giving direct evidence that the α7 receptor is necessary to maintain the tonic inhibitory influence of the cholinergic anti-inflammatory pathway. Signal transduction mechanisms involving the α7nAChR are an area of active study by a number of groups and more data are needed to fully understand this mechanism. There is general agreement that the cytokine suppressing signals from α7nAChR are not dependent upon activation of ion channels, the principal mechanism, by which α7nAChR mediates signalling in neurons. Rather, the current signal transduction model indicates that receptor ligand interaction activates JAK-STAT dependent inhibition of the nuclear translocation of nuclear factor (NF)-κB, resulting in decreased transcription of cytokine genes [22–24].

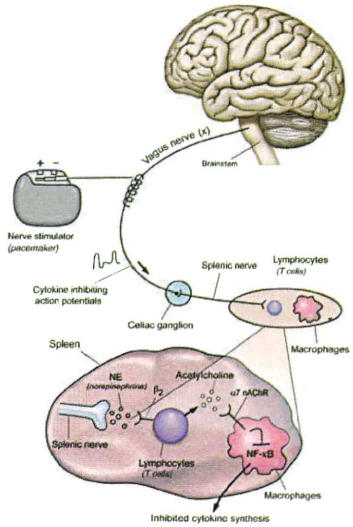

Fig. 1 *Action potentials transiting the vagus nerve synapse in the coeliac ganglion, the origin of the splenic nerve. The splenic nerve controls lymphocytes in the spleen, which can produce acetylcholine that interacts with α7 nicotinic acetylcholine receptors expressed on cytokine producing macrophages. Intracellular signal transduction through this receptor inhibits the activity of nuclear factor-κB to suppress cytokine production. Nerve stimulators can provide an identical signal to initiate the anti-inflammatory pathway, an approach that reverse signs and symptoms in preclinical disease models of arthritis, inflammatory bowel disease, ischaemia-reperfusion injury, heart failure, pancreatitis, sepsis and other syndromes.*

Organs of the reticuloendothelial system, including the lungs, liver and spleen, contain innate immune cells that mediate the immediate, early response to pathogens and injury. During endotoxemia, an experimental model of Gram-negative bacterial shock produced by administration of lipopolysaccharide, the spleen is the major organ source of systemic TNF that accumulates in blood [7, 25]. TNF production in spleen accounts for >90% of the total TNF burden that reaches the circulation, so it is perhaps not surprising that splenectomy significantly reduces circulating TNF levels in endotoxin-challenged mice. Vagus nerve stimulation fails to inhibit systemic TNF production in splenectomized mice or in mice following interruption of either the common coeliac branch of the abdominal vagus nerve, or the splenic nerve, indicating that cholinergic anti-inflammatory pathway control of TNF culminates in spleen [7, 26, 27]. As expected by the observation that vagus nerve stimulation suppresses serum TNF, vagus nerve stimulation significantly reduces TNF synthesis in spleen, an effect that requires α7nAChR. Moreover, administration of selective α7nAChR agonists to splenectomized mice fails to reduce cytokine levels; rather, this exacerbates pro-inflammatory cytokine production and increases lethality [7, 13, 25]. These findings indicate that the spleen is a critical physiological interface between cholinergic anti-inflammatory signalling and regulation of systemic immune responses.

In addition to regulating cytokine release, the cholinergic anti-inflammatory pathway modulates the expression of activation markers on circulating leukocytes that transit the spleen. Vagus nerve stimulation down-regulates neutrophil activation by attenuating expression of CD11b, a surface molecule required for cell adhesion and chemotaxis [28]. The mechanism of CD11b suppression requires F-actin polymerization, the rate-limiting step for CD11b surface expression. Using a carrageenan air pouch

model to study recruitment of neutrophils to sites of local soft tissue inflammation, stimulating the vagus nerve significantly inhibits neutrophil recruitment [28, 29]. An intact spleen is required for this response because vagus nerve stimulation of splenectomized animals fails to inhibit neutrophil recruitment to the air pouch [25, 28]. In the absence of exogenous vagus nerve stimulation, removing the spleen also interferes with endogenous neutrophil trafficking. These results indicate that vagus nerve signals to spleen control the activity of circulating immune cells, regulating the ability of these cells to respond to inflammatory stimuli and migrate to local zones of ongoing inflammation, even when these regions are not innervated directly by the vagus nerve. Together these findings point to a specific, centralized neural pathway innervating the spleen that is positioned to both suppress inflammatory cytokine production and downregulate the activity of circulating inflammatory cells.

It is interesting to consider the clinical experience with splenectomized patients. Even with the availability of effective vaccines, splenectomized patients are at increased risk for potentially lethal bacterial infections from the syndrome of overwhelming postsplenectomy sepsis. The pathogenesis of this syndrome is debated, but it has been attributed to inadequate immune responsiveness, particularly to encapsulated bacteria [30]. Based on these new insights provided by the cholinergic anti-inflammatory pathway, it is intriguing to consider whether patients dying of postsplenectomy complications develop uncontrolled, and ultimately lethal, cytokine responses due to the absence of a functional inflammatory reflex.

Central activation of the cholinergic anti-inflammatory pathway

The original concept of the inflammatory reflex followed experimental observations that administration of extremely low quantities of CNI-1493 into the brain inhibited systemic TNF production during endotoxemia [31]. This effect was not attributable to either leakage of the drug from the brain into the periphery, or to stimulation of the hypothalamic-pituitary-adrenal axis. Surprisingly at the time, the systemic cytokine inhibitory actions of intracerebral CNI-1493 were dependent upon the vagus nerve because vagotomy abolished the TNF-suppressing effects of intracerebral administration [9]. This was ultimately explained by the fact that CNI-1493 is a weak agonist of the M1 class of muscarinic receptors, which stimulate activity within descending forebrain cholinergic neural pathways that mediate increased efferent vagus nerve activity [32, 33]. Intracerebral M1 muscarinic receptors had been implicated in the control of visceral functions by the vagus nerve, including glycogen synthesis in the liver, pancreatic exocrine secretion and cardiovascular reflexes [34, 35]. Administration of selective muscarinic receptor agonists into the brain stimulates vagus nerve mediated suppression of cytokine production during endotoxemia [32, 33]. These effects are directly attributable to intracerebral signals because peripheral administration of muscarinic receptor agonists that cannot cross the blood-brain barrier fails to inhibit cytokine release. There is now widespread interest in studying the anti-inflammatory effects of clinically approved, centrally acting acetylcholinesterase inhibitors, which increase brain acetylcholine levels and enhance M1 signalling. Preclinical studies indicate that these agents increase the activity of the cholinergic anti-inflammatory pathway and suppress inflammation in the periphery. It may be possible to exploit this approach in clinical trials of treating inflammatory diseases, including rheumatoid arthritis, inflammatory bowel disease and psoriasis because these diseases can be controlled by inhibiting cytokine activity.

Clinical implications of the inflammatory reflex

Neural circuits function reflexively to maintain physiological stability in visceral organs. Each reflex is comprised of a sensory or afferent arc that detects environmental and chemical changes. This information is relayed to neural centres in the central nervous system, which integrate the input and relay neural signals to an output or motor nucleus. Efferent signals are then relayed by motor neurons travelling to the innervated organ to produce a response that maintains an 'appropriate' or healthy level of function. The net physiological effect of this reflexive behaviour is a system output that varies according to a set point function curve. For example, consider the control of heart rate: increases in heart rate activate a reflex circuit that leads to increased activity in the vagus nerve, which slows heart rate and restores homoeostasis. A major unanswered question in clinical immunology is whether it is possible to record neural activity in the vagus nerve as a surrogate marker of activity in the inflammatory reflex to determine the sensitivity of the innate immune system to inflammation.

Measuring vagus nerve activity: Heart rate variability

A widely used approach to measuring vagus nerve activity in humans is based on cardiac physiology.

Heart rate is controlled by action potentials transmitted via the vagus nerve to the sinoatrial node of the heart, where vagus nerve-dependent acetylcholine release essentially 'prolongs' the time to the next heartbeat, thus slowing the pulse. Measuring the time between individual hearts beats, as can be accomplished with software that captures the distance between R waves on the electrocardiogram (EKG) tracing, provides information about the instantaneous heart rate. These data are then plotted as a function of time to provide analysis of heart rate variability (HRV), or the dynamic variation of heart rate under control of the sympathetic and parasympathetic nervous input [36]. Heart rate variability represents the time differences between successive heartbeats (also known as the beat-to-beat interval), and is synonymous with RR variability, referring to the R waves on the electrocardiogram corresponding to ventricular depolarization.

Analysis of the time differences between successive heartbeats to assess HRV can be accomplished with reference to time (time domain analysis) or frequency (frequency domain analysis). The former is based on the normal-to-normal (NN) interval, or the time difference between successive QRS complexes (RR interval) resulting from sinus node depolarization on a standard, continuous EKG. Statistical analysis of measurements of the NN intervals, or those derived from the differences between NN intervals yields various measures of inter-beat variability. Examples include the standard deviation of the NN interval, i.e. the square root of variance, the standard deviation of the average NN interval calculated over short periods and the square root of the mean squared differences of successive NN intervals >50 ms.

Frequency domain analysis, which is more widely used to analyse HRV, utilizes spectral methods to interpret the RR tachogram. Power spectral density analysis provides information of how power (variability) distributes as a function of frequency. A mathematical algorithm, Fast fourier transform, generates spectral (frequency) components that are labelled ultra-low frequency (ULF), very low frequency (VLF), low frequency (LF) and high frequency (HF) power components. Power components can be expressed in absolute values (ms^2) or in normalized units, which are used to represent the relative contribution of each power component to the total variance (power) in the recording.

Extensive physiological and pharmacological studies have examined the neural contributions to the frequency components of HRV. For example, administration of acetylcholine antagonists or vagotomy down modulates the HF power component and electrical vagus nerve stimulation increases HF power [37]. These results indicate that the HF power component reflects efferent vagus nerve activity to the sinoatrial node. The interpretation of LF power is less clear, but most agree that the LF component is a measure of sympathetic activity or a combination of sympathetic and parasympathetic activity [37]. The ratio of low-to-high- frequency spectral power (LF/HF) has been proposed as an index of sympathetic to parasympathetic balance of heart rate fluctuation. A consensus has not been achieved concerning the physiological correlates of VLF and ULF power.

Measures of HRV have been strongly correlated to morbidity and mortality from diverse diseases. Early clinical findings, first observed more than 50 years ago, revealed that variability in RR intervals predict the onset of foetal distress before any measurable changes in absolute heart rate [38–40]. There is now extensive experience using HRV measures in diverse disease syndromes and these data indicate that decreased vagus nerve activity is associated with increased morbidity and mortality. These correlations include increased morbidity and mortality following cardiac surgery or myocardial infarction, increased mortality from sepsis and progression or disease severity in autoimmune diseases, including rheumatoid arthritis, inflammatory bowel disease, systemic lupus erythematosus and sarcoidosis [41–49]. Prior to knowledge of the inflammatory reflex, it was thought that decreased vagus nerve activity in these cases resulted from neural damage associated with the underlying diseases. It is now possible to consider an alternative explanation that decreased vagus nerve activity and the associated loss of the tonic inhibitory influence of the cholinergic anti-inflammatory pathway on innate immune responses and cytokine release, may enable significantly enhanced cytokine responses to stimuli that would have been otherwise harmless in the presence of a functioning neural circuit.

Planned and ongoing clinical studies in patients with cytokine-mediated diseases, including rheumatoid arthritis, inflammatory bowel disease, sepsis, psoriasis and depression are providing new insights into measures of vagus nerve activity as a direct correlate to cholinergic anti-inflammatory pathway activity. We recently assessed RR interval variability in rheumatoid arthritis and observed that vagus nerve activity was significantly decreased in patients as com-

pared with healthy controls [50, 51] Moreover, serum levels of HMGB1, a cytokine that has been implicated in the pathogenesis of rheumatoid arthritis and other inflammatory syndromes, are significantly related to RR interval variability. There was no significant relationship between disease severity and vagus nerve activity, which is consistent with the hypothesis that impaired vagus nerve activity, is not the result of advancing disease. Vagus nerve activity was predictive of the innate immune response to endotoxin and administration of endotoxin to healthy human subjects revealed a significant correlation of basal high-frequency variability to the magnitude of TNF release [52]. Together these results support the hypothesis that diminished vagus nerve signals, which normally provide an inhibitory influence on cytokine production, which contribute to enhanced or unregulated production of TNF and other inflammatory mediators.

Depressed vagus nerve activity has been implicated in exaggerated inflammation in peripheral organs following brain death, and as expected, HRV decreases significantly following brain death in rats [53]. Interestingly, before harvesting donor organs, vagus nerve stimulation significantly decreases cytokine concentrations in serum and reduces the expression of pro-inflammatory cytokines, E-selectin, IL-1β and ITGA6. Moreover, assessment of renal function reveals significant improvements in recipients of grafts from donors, who had been subjected to vagus nerve stimulation as compared with unstimulated donor grafts [53]. These results agree with a direct, contributory role of impaired vagus nerve signalling in excessive cytokine release during ischaemia before organ harvesting.

Numerous studies have investigated the relationship between depression, systemic cytokine production and HRV. Depression is associated with abnormalities in innate and adaptive immune function, including increased production of pro-inflammatory cytokines, decreased production of anti-inflammatory cytokines and increased expression of surface markers associated with immune cell activation [54–56]. It is plausible that over-expression of cytokines in the brain may influence depressive behaviour because cognitive impairment, behavioural dysfunction and sickness syndrome effects are mediated by cytokines, including TNF. Current data are unable to determine whether the onset of a major depressive episode precedes the development of a dysfunctional immune response, or *vice versa*. Patients with major depressive disorder also exhibit decreased HRV and the severity of the impairment correlates with the clinical severity of depression [57]. Moreover, implantable vagus nerve stimulators are used in patients with treatment-resistant depression, with improvements observed in a significant percentage of patients [58–60]. It is now interesting to consider whether these observations regarding the relationship between depression and maladaptive immune responses result from impaired vagus nerve regulation of cytokine release. It should be possible to design clinical studies to address the question of whether increasing vagus nerve activity using a nerve stimulator corrects the dysregulated cytokine response and lowers the exposure of the brain to cytokines that disrupt behaviour. End point selection of these studies will be is critically important and should include assays of stimulated cytokine release (e.g. whole blood endotoxin stimulated cytokine release) because basal cytokine levels are not well correlated to disease severity [61].

The role of inflammation in the development and progression of atherosclerosis is another area of significant interest and a number of recent studies have explored the potential relationship between the inflammatory reflex and atherogenic risk [62–65]. For example, C-reactive protein (CRP), implicated as an independent risk factor for cardiovascular mortality and morbidity, was measured in 678 healthy subjects. CRP levels were significantly inversely related with vagus nerve activity, as assessed by HRV, thus providing clinical evidence that vagus nerve activity may modulate systemic inflammatory responses in cardiovascular disease [36]. Another large study of CRP and IL-6 levels was conducted in 682 outpatients with coronary heart disease and vagus nerve activity was inversely correlated with CRP and IL-6 levels [66]. The relationship between circulating inflammatory markers has also been studied in healthy university students, (20.56 ± 0.82 years) and those subjects in the highest tertile of hs-CRP had significantly decreased vagus nerve activity [67]. Moreover, vagus nerve activity was inversely correlated with hs-CRP, with the lowest hs-CRP levels observed in the most physically active subjects, who also had the highest levels of vagus nerve activity. Thus, loss of the inflammation suppressing activity of vagus nerve signals may contribute to overproduction of CRP, which in turn is controlled by cytokines, including IL-1 and IL-6.

Sloan *et al.* [68] recently assessed whether aerobic exercise training can modulate vagus nerve activity and whole blood production of TNF. In a study of 61 healthy sedentary subjects (age 20–45 year), those

receiving the highest intensity aerobic training had significant reductions in TNF production. These data suggest that in healthy young adults, a 12-week high-intensity aerobic training programme, sufficient to increase VO_2 max, can inhibit cytokine release from blood monocytes. A larger study is presently underway to assess the role of vagus nerve activity in conferring protection against inflammatory cytokine release in humans [68]. It has been proposed that a major cardio-protective benefit of exercise is derived from enhanced vagus nerve activity, which inhibits inflammatory risk and atherogenesis.

There is a need to determine whether augmenting vagus nerve activity in patients who are deficient in this activity will reduce cytokine production and the levels of other inflammatory factors, including CRP and IL-6. This has not been reported in patients with autoimmune or other active inflammatory diseases, but a study of 183 healthy adults (mean age = 45) revealed that higher vagus nerve activity is significantly associated with lower production of TNF and IL-6 in endotoxin- stimulated whole blood assays [69]. This association was independent of demographical and health characteristics, including age, gender, race, years of education, smoking, hypertension and white blood cell count. These authors concluded that vagus nerve activity is inversely related to the activity of inflammatory mediators, which has potential implications for studying mechanisms linking psychosocial factors to risk for inflammatory diseases.

Are the cardiac and immune regulatory vagus nerve pathways linked?

As clinical studies of vagus nerve- mediated inflammatory responses expand, it may be possible to dissociate the neural pathways that regulate immunity from those that regulate other vagus nerve functions. In animal studies of direct stimulation of the vagus nerve, it is possible to activate the cholinergic anti-inflammatory pathway by delivering an electrical charge that is below the threshold required to significantly change heart rate [13]. Thus, the neural tracts descending in the vagus nerve to modulate immune responses function at a lower firing threshold than the cardio-inhibitory fibres. It is likely that there are anatomical and physiological differences that underlie these responses. For example, cardio-inhibitory vagus nerve fibres in mammals are B and C fibre types, which require significantly higher stimulation intensities to fire as compared with myelinated A-type fibres, which do not participate in heart rate regulation. These 'lower threshold' A signalling fibres may convey the anti-inflammatory signal of the cholinergic anti-inflammatory pathway to peripheral immune cells [13].

The relationship between activation thresholds of the cholinergic anti-inflammatory pathway and regulation of HRV is an area of intensive study and the available clinical evidence indicates that when vagus nerve activity is deficient, inflammation is excessive. There are theoretical and practical advantages to developing devices that can selectively activate the cholinergic anti-inflammatory pathway without stimulating cardiac fibres. It may be possible to draw correlative analysis from measurements of HRV to identify individuals with reduced vagus nerve signalling, who are susceptible to tissue damage from inflammation. Heart rate variability could serve as a biomarker to identify patients, who may benefit from pharmacological or electrical stimulation of the cholinergic anti-inflammatory pathway. As Holter monitors are used to track changes in heart rhythm, HRV monitors may one day provide indices of diminished or enhanced vagus anti-inflammatory activity. During therapy for inflammation, it may be possible to measure the physiological level of exogenous cholinergic stimulation delivered to each patient and to modulate the delivery of therapy by altering voltage, pulse and time in order to tailor the treatment to the individual, based on changes in HRV. Autoimmune diseases are characterized by waxing and waning clinical episodes and HRV measurements may one - day be used to predict impending relapse by revealing declining activity in the cholinergic anti-inflammatory pathway, thus signalling the need for additional treatment to enhance the neural network.

It is also theoretically possible that monitoring HRV and vagus nerve activity may prove to be useful as a long-term measure of inflammation in chronic diseases. Similar to tracking haemoglobin A1c levels in patients with diabetes, or daily blood pressure monitoring in patients with hypertension, HRV monitoring could theoretically be developed to monitor the activity of inflammatory risk in these and other cytokine-mediated diseases. Noninvasive methods to determine HRV are available and it will be of interest to assess the usefulness of portable monitoring devices at home that interface with central monitoring stations to provide online analysis of changes in the inflammatory reflex. Correction of chronic, maladaptive levels of inflammation using nerve stimulators might prevent the progression of debilitating and deadly diseases, potentially replacing the need for some biological therapeutics.

Acknowledgements

Supported in part by grants from the NIH (NIGMS) to KJT.

Conflict of interest statement

No conflict of interest was declared.

References

1 Lotze MT, Tracey KJ. High-mobility group box 1 protein (HMGB1): nuclear weapon in the immune arsenal. *Nat Rev Immunol* 2005; **5:** 331–42.
2 Yang H, Hreggvidsdottir HS, Palmblad K *et al.* A Critical Cysteine is Required for HMGB1 Binding to TLR4 and Activation of Macrophage Cytokine Release. *Proc Natl Acad Sci USA* 2010; **26:** 11942–7.
3 Medzhitov R. Inflammation 2010: new adventures of an old flame. *Cell* 2010; **140:** 771–6.
4 Borovikova LV, Ivanova S, Nardi D *et al.* Role of vagus nerve signaling in CNI-1493-mediated suppression of acute inflammation. *Auton Neurosci* 2000; **85:** 141–7.
5 Borovikova LV, Ivanova S, Zhang M *et al.* Vagus nerve stimulation attenuates the systemic inflammatory response to endotoxin. *Nature* 2000; **405:** 458–62.
6 Tracey KJ. The inflammatory reflex. *Nature* 2002; **420:** 853–9.
7 Huston JM, Ochani M, Rosas-Ballina M *et al.* Splenectomy inactivates the cholinergic antiinflammatory pathway during lethal endotoxemia and polymicrobial sepsis. *J Exp Med* 2006; **203:** 1623–8.
8 Wang H, Yu M, Ochani M *et al.* Nicotinic acetylcholine receptor alpha7 subunit is an essential regulator of inflammation. *Nature* 2003; **421:** 384–8.
9 Bernik TR, Friedman SG, Ochani M *et al.* Pharmacological stimulation of the cholinergic antiinflammatory pathway. *J Exp Med* 2002; **195:** 781–8.
10 Bernik TR, Friedman SG, Ochani M *et al.* Cholinergic antiinflammatory pathway inhibition of tumor necrosis factor during ischemia reperfusion. *J Vasc Surg* 2002; **36:** 1231–6.
11 van Westerloo DJ, Giebelen IA, Florquin S *et al.* The vagus nerve and nicotinic receptors modulate experimental pancreatitis severity in mice. *Gastroenterology* 2006; **130:** 1822–30.
12 van Westerloo DJ, Giebelen IA, Florquin S *et al.* The cholinergic anti-inflammatory pathway regulates the host response during septic peritonitis. *J Infect Dis* 2005; **191:** 2138–48.
13 Huston JM, Gallowitsch-Puerta M, Ochani M *et al.* Transcutaneous vagus nerve stimulation reduces serum high mobility group box 1 levels and improves survival in murine sepsis. *Crit Care Med* 2007; **35:** 2762–8.
14 Yeboah MM, Xue X, Duan B *et al.* Cholinergic agonists attenuate renal ischemia-reperfusion injury in rats. *Kidney Int* 2008; **74:** 62–9.
15 van Maanen MA, Lebre MC, van der PT *et al.* Stimulation of nicotinic acetylcholine receptors attenuates collagen-induced arthritis in mice. *Arthritis Rheum* 2009; **60:** 114–22.
16 Mioni C, Bazzani C, Giuliani D *et al.* Activation of an efferent cholinergic pathway produces strong protection against myocardial ischemia/reperfusion injury in rats. *Crit Care Med* 2005; **33:** 2621–8.
17 Guarini S, Cainazzo MM, Giuliani D *et al.* Adrenocorticotropin reverses hemorrhagic shock in anesthetized rats through the rapid activation of a vagal anti-inflammatory pathway. *Cardiovasc Res* 2004; **63:** 357–65.
18 Guarini S, Altavilla D, Cainazzo MM *et al.* Efferent vagal fibre stimulation blunts nuclear factor-kappaB activation and protects against hypovolemic hemorrhagic shock. *Circulation* 2003; **107:** 1189–94.
19 Ottani A, Giuliani D, Galantucci M *et al.* Melanocortins counteract inflammatory and apoptotic responses to prolonged myocardial ischemia/reperfusion through a vagus nerve-mediated mechanism. *Eur J Pharmacol* 2010; **637:** 124–30.
20 Li J, Xie H, Wen T, Liu H, Zhu W, Chen X. Expression of high mobility group box chromosomal protein 1 and its modulating effects on downstream cytokines in systemic lupus erythematosus. *J Rheumatol* 2010; **37:** 766–75.
21 Tracey KJ. Understanding immunity requires more than immunology. *Nat Immunol* 2010; **11:** 561–4.
22 Parrish WR, Rosas-Ballina M, Gallowitsch-Puerta M *et al.* Modulation of TNF Release by Choline Requires Alpha7 Subunit Nicotinic Acetylcholine Receptor-Mediated Signaling. *Mol Med* 2008; **14:** 567–74.
23 de Jonge WJ, van der Zanden EP, The FO *et al.* Stimulation of the vagus nerve attenuates macrophage activation by activating the Jak2-STAT3 signaling pathway. *Nat Immunol* 2005; **6:** 844–51.
24 Wang H, Liao H, Ochani M *et al.* Cholinergic agonists inhibit HMGB1 release and improve survival in experimental sepsis. *Nat Med* 2004; **10:** 1216–21.
25 Huston JM, Wang H, Ochani M *et al.* Splenectomy protects against sepsis lethality and reduces serum HMGB1 levels. *J Immunol* 2008; **181:** 3535–9.
26 Rosas-Ballina M, Tracey KJ. The neurology of the immune system: neural reflexes regulate immunity. *Neuron* 2009; **64:** 28–32.
27 Rosas-Ballina M, Ochani M, Parrish WR *et al.* Splenic nerve is required for cholinergic antiinflammatory pathway control of TNF in endotoxemia. *Proc Natl Acad Sci USA* 2008; **105:** 11008–13.
28 Huston JM, Rosas-Ballina M, Xue X *et al.* Cholinergic neural signals to the spleen down-regulate leukocyte trafficking via CD11b. *J Immunol* 2009; **183:** 552–9.
29 Saeed RW, Varma S, Peng-Nemeroff T *et al.* Cholinergic stimulation blocks endothelial cell activation and leukocyte recruitment during inflammation. *J Exp Med* 2005; **201:** 1113–23.
30 Brigden ML, Pattullo AL. Prevention and management of overwhelming postsplenectomy infection–an update. *Crit Care Med* 1999; **27:** 836–42.
31 Tracey KJ. Suppression of TNF and other proinflammatory cytokines by the tetravalent guanylhydrazone CNI-1493. *Prog Clin Biol Res* 1998; **397:** 335–43.
32 Pavlov VA, Parrish WR, Rosas-Ballina M *et al.* Brain acetylcholinesterase activity controls systemic cytokine levels through the cholinergic anti-inflammatory pathway. *Brain Behav Immun* 2009; **23:** 41–5.
33 Pavlov VA, Ochani M, Gallowitsch-Puerta M *et al.* Central muscarinic cholinergic regulation of the systemic inflammatory response during endotoxemia. *Proc Natl Acad Sci USA* 2006; **103:** 5219–23.
34 Li Y, Wu X, Zhu J, Yan J, Owyang C. Hypothalamic regulation of pancreatic secretion is mediated by central cholinergic pathways in the rat. *J Physiol* 2003; **552:** 571–87.
35 Shimazu T, Matsushita H, Ishikawa K. Cholinergic stimulation of the rat hypothalamus: effects of liver glycogen synthesis. *Science* 1976; **194:** 535–6.

36 Sloan RP, McCreath H, Tracey KJ, Sidney S, Liu K, Seeman T. RR interval variability is inversely related to inflammatory markers: the CARDIA study. *Mol Med* 2007; **13:** 178–84.
37 Heart rate variability: standards of measurement, physiological interpretation and clinical use. Task Force of the European Society of Cardiology and the North American Society of Pacing and Electrophysiology. *Circulation* 1996; **93:** 1043–65.
38 Gaziano EP, Freeman DW. Analysis of heart rate patterns preceding fetal death. *Obstet Gynecol* 1977; **50:** 578–82.
39 Sampson MB, Mudaliar NA, Lele AS. Fetal heart rate variability as an indicator of fetal status. *Postgrad Med* 1980; **67:** 207–10, 213–15.
40 Lauersen NH, Wilson KH, Bilek A, Rao VS, Kurkulos M. A new modality in nonstress testing: evaluation of beat-to-beat fetal heart rate variability. *Am J Obstet Gynecol* 1981; **141:** 521–6.
41 Kleiger RE, Miller JP, Bigger JT Jr, Moss AJ. Decreased heart rate variability and its association with increased mortality after acute myocardial infarction. *Am J Cardiol* 1987; **59:** 256–62.
42 La Rovere MT, Bigger JT Jr, Marcus FI, Mortara A, Schwartz PJ. Baroreflex sensitivity and heart-rate variability in prediction of total cardiac mortality after myocardial infarction. ATRAMI (Autonomic Tone and Reflexes After Myocardial Infarction) Investigators. *Lancet* 1998; **351:** 478–84.
43 Schwartz PJ, La Rovere MT, Vanoli E. Autonomic nervous system and sudden cardiac death. Experimental basis and clinical observations for post-myocardial infarction risk stratification. *Circulation* 1992; **85:** I77–91.
44 Garrard CS, Kontoyannis DA, Piepoli M. Spectral analysis of heart rate variability in the sepsis syndrome. *Clin Auton Res* 1993; **3:** 5–13.
45 Schmidt H, Muller-Werdan U, Hoffmann T *et al.* Autonomic dysfunction predicts mortality in patients with multiple organ dysfunction syndrome of different age groups. *Crit Care Med* 2005; **33:** 1994–2002.
46 Aydemir M, Yazisiz V, Basarici I *et al.* Cardiac autonomic profile in rheumatoid arthritis and systemic lupus erythematosus. *Lupus* 2010; **19:** 255–61.
47 Stojanovich L, Milovanovich B, de Luka SR *et al.* Cardiovascular autonomic dysfunction in systemic lupus, rheumatoid arthritis, primary Sjogren syndrome and other autoimmune diseases. *Lupus* 2007; **16:** 181–5.
48 Sharma P, Makharia GK, Ahuja V, Dwivedi SN, Deepak KK. Autonomic dysfunctions in patients with inflammatory bowel disease in clinical remission. *Dig Dis Sci* 2009; **54:** 853–61.
49 Lindgren S, Stewenius J, Sjolund K, Lilja B, Sundkvist G. Autonomic vagal nerve dysfunction in patients with ulcerative colitis. *Scand J Gastroenterol* 1993; **28:** 638–42.
50 Bruchfeld A, Goldstein RS, Chavan S *et al.* Whole blood cytokine attenuation by cholinergic agonists ex vivo and relationship to vagus nerve activity in rheumatoid arthritis. *J Intern Med* 2010; **268:** 94–101.
51 Goldstein RS, Bruchfeld A, Yang L *et al.* Cholinergic anti-inflammatory pathway activity and High Mobility Group Box-1 (HMGB1) serum levels in patients with rheumatoid arthritis. *Mol Med* 2007; **13:** 210–5.
52 Jan BU, Coyle SM, Macor MA, Reddell M, Calvano SE, Lowry SF. Relationship of basal heart rate variability to *in vivo* cytokine responses after endotoxin exposure. *Shock* 2010; **33:** 363–8.
53 Hoeger S, Bergstraesser C, Selhorst J *et al.* Modulation of brain dead induced inflammation by vagus nerve stimulation. *Am J Transplant* 2010; **10:** 477–89.
54 Dantzer R, O'Connor JC, Freund GG, Johnson RW, Kelley KW. From inflammation to sickness and depression: when the immune system subjugates the brain. *Nat Rev Neurosci* 2008; **9:** 46–56.
55 Raison CL, Capuron L, Miller AH. Cytokines sing the blues: inflammation and the pathogenesis of depression. *Trends Immunol* 2006; **27:** 24–31.
56 Miller AH, Maletic V, Raison CL. Inflammation and its discontents: the role of cytokines in the pathophysiology of major depression. *Biol Psychiatry* 2009; **65:** 732–41.
57 Kemp AH, Quintana DS, Gray MA, Felmingham KL, Brown K, Gatt JM. Impact of depression and antidepressant treatment on heart rate variability: a review and meta-analysis. *Biol Psychiatry* 2010; **67:** 1067–74.
58 Bajbouj M, Merkl A, Schlaepfer TE *et al.* Two-year outcome of vagus nerve stimulation in treatment-resistant depression. *J Clin Psychopharmacol* 2010; **30:** 273–81.
59 Rush AJ, Sackeim HA, Marangell LB *et al.* Effects of 12 months of vagus nerve stimulation in treatment-resistant depression: a naturalistic study. *Biol Psychiatry* 2005; **58:** 355–63.
60 Marangell LB, Rush AJ, George MS *et al.* Vagus nerve stimulation (VNS) for major depressive episodes: one year outcomes. *Biol Psychiatry* 2002; **51:** 280–7.
61 Dowlati Y, Herrmann N, Swardfager W *et al.* A meta-analysis of cytokines in major depression. *Biol Psychiatry* 2010; **67:** 446–57.
62 Lampert R, Bremner JD, Su S *et al.* Decreased heart rate variability is associated with higher levels of inflammation in middle-aged men. *Am Heart J* 2008; **156:** 759.e1–7.
63 Haensel A, Mills PJ, Nelesen RA, Ziegler MG, Dimsdale JE. The relationship between heart rate variability and inflammatory markers in cardiovascular diseases. *Psychoneuroendocrinology* 2008; **33:** 1305–12.
64 Carney RM, Freedland KE, Stein PK *et al.* Heart rate variability and markers of inflammation and coagulation in depressed patients with coronary heart disease. *J Psychosom Res* 2007; **62:** 463–7.
65 Janszky I, Ericson M, Lekander M *et al.* Inflammatory markers and heart rate variability in women with coronary heart disease. *J Intern Med* 2004; **256:** 421–8.
66 Frasure-Smith N, Lesperance F, Irwin MR, Talajic M, Pollock BG. The relationships among heart rate variability, inflammatory markers and depression in coronary heart disease patients. *Brain Behav Immun* 2009; **23:** 1140–7.
67 Soares-Miranda L, Negrao CE, Antunes-Correa LM *et al.* High levels of C-reactive protein are associated with reduced vagal modulation and low physical activity in young adults. *Scand J Med Sci Sports* 2010; July 6. [Epub ahead of Print].
68 Sloan RP, Shapiro PA, Demeersman RE *et al.* Aerobic exercise attenuates inducible TNF production in humans. *J Appl Physiol* 2007; **103:** 1007–11.
69 Marsland AL, Gianaros PJ, Prather AA, Jennings JR, Neumann SA, Manuck SB. Stimulated production of proinflammatory cytokines covaries inversely with heart rate variability. *Psychosom Med* 2007; **69:** 709–16.

Correspondence: Jared M. Huston, MD, Department of Surgery, Stony Brook University Medical Center, T18-040, Health Sciences Center, Stony Brook, NY 11794, USA.
([fax: +631-444-6176; e-mail: jhuston@notes.cc.sunysb.edu).](mailto:jhuston@notes.cc.sunysb.edu))

OPEN ACCESS Freely available online

PLoS one

The Prognostic Value of Non-Linear Analysis of Heart Rate Variability in Patients with Congestive Heart Failure—A Pilot Study of Multiscale Entropy

Yi-Lwun Ho[1,2], Chen Lin[3,4,5], Yen-Hung Lin[2], Men-Tzung Lo[3,4]*

1 Graduate Institute of Clinical Medicine, National Taiwan University Hospital and National Taiwan University College of Medicine, Taipei, Taiwan, **2** Division of Cardiology, Department of Internal Medicine, National Taiwan University Hospital and National Taiwan University College of Medicine, Taipei, Taiwan, **3** Center for Dynamical Biomarkers and Translational Medicine, National Central University, Chungli, Taiwan, **4** Research Center for Adaptive Data Analysis, National Central University, Taoyuan, Taiwan, **5** Institute of Systems Biology and Bioinformatics, National Central University, Taoyuan, Taiwan

Abstract

Aims: The influences of nonstationarity and nonlinearity on heart rate time series can be mathematically qualified or quantified by multiscale entropy (MSE). The aim of this study is to investigate the prognostic value of parameters derived from MSE in the patients with systolic heart failure.

Methods and Results: Patients with systolic heart failure were enrolled in this study. One month after clinical condition being stable, 24-hour Holter electrocardiogram was recording. MSE as well as other standard parameters of heart rate variability (HRV) and detrended fluctuation analysis (DFA) were assessed. A total of 40 heart failure patients with a mea age of 56±16 years were enrolled and followed-up for 684±441 days. There were 25 patients receiving β-blockers treatment. During follow-up period, 6 patients died or received urgent heart transplantation. The short-term exponent of DFA and the slope of MSE between scale 1 to 5 were significantly different between patients with or without β-blockers ($p = 0.014$ and $p = 0.028$). Only the area under the MSE curve for scale 6 to 20 ($Area_{6-20}$) showed the strongest predictive power between survival ($n = 34$) and mortality ($n = 6$) groups among all the parameters. The value of $Area_{6-20} \leq 21.2$ served as a significant predictor of mortality or heart transplant ($p = 0.0014$).

Conclusion: The area under the MSE curve for scale 6 to 20 is not relevant to β-blockers and could further warrant independent risk stratification for the prognosis of CHF patients.

Citation: Ho Y-L, Lin C, Lin Y-H, Lo M-T (2011) The Prognostic Value of Non-Linear Analysis of Heart Rate Variability in Patients with Congestive Heart Failure—A Pilot Study of Multiscale Entropy. PLoS ONE 6(4): e18699. doi:10.1371/journal.pone.0018699

Editor: Matjaz Perc, University of Maribor, Slovenia

Received December 31, 2010; **Accepted** March 8, 2011; **Published** April 13, 2011

Funding: M-T Lo was supported by NSC (Taiwan, ROC), Grant No 99-2627-B-008-003, joint foundation of CGH and NCU, Grant No CNJRF-99CGH-NCU-A3, VGHUST100-G1-4-3 and NSC support for the Center for Dynamical Biomarkers and Translational Medicine, National Central University, Taiwan (NSC 99-2911-I-008-100). The funders had no role in study design, data collection and analysis, decision to publish, or preparation of the manuscript.

Competing Interests: The authors have declared that no competing interests exist.

* E-mail: mzlo@ncu.edu.tw

Introduction

Congestive heart failure (CHF) remains to be one of the major cardiovascular disorders in the world [1]. Despite its high expenditure in healthcare budgets [2], the mortality rate of CHF patients can be up to 8 times higher than the age-matched control population [3]. The present treatment protocols of CHF patients, such as administrating angiotensin converting enzyme inhibitors (ACE-I) and β blockers, have been proven to lower the mortality and hospital admission rate [4]. Nevertheless, the residual risk for mortality and morbidity of CHF remains high even under such treatment protocols [5,6]. Therefore, further novel prognostic predictor is needed to strengthen the treatment strategy in addition to neurohormonal inhibition therapy.

Conventional linear heart rate variability (HRV) analyses, including frequency and time domain analyses, have been reported as prognostic factors for CHF [7,8]. However, heart rate fluctuations have been recognized as complex behaviors originated from nonlinear processes and often with nonstationary property [9–11]. Applying linear algorithms to those seemingly irregular and "patchy" patterns of heart rate fluctuations [12] may cause the intrinsic computational errors of the linear algorithms [11,13,14]. Properly use of the analyses based on fractals and chaos theory [15–17] to qualify or quantify the characteristics of heart rate time series are suggested to serve as a more reliable index of physiological systems in many clinical studies [10,11,18]. As one of such mathematic methods, multiscale entropy (MSE) analysis has focused specifically on characterizing heterogeneous complexity [19]. Such complex structure is "breakdown" (loss of information richness) and points to poor prognosis in CHF patients [19,20]. We hypothesized that MSE could yield a prognostic marker which was not relevant to neurohormonal inhibition therapy in CHF patients. The aims of this study were 1) to evaluate the influences of β-blockers on parameters derived from MSE; 2) to assess the prognostic significance of parameters derived from MSE for CHF patients.

Methods

Study Population

Patients with manifestation of exertional dyspnea, leg edema and systolic heart failure (LVEF<45% by echocardiography) at the National Taiwan University Hospital were enrolled after giving their inform consents. Baseline information, including age, sex, etiologies for heart failure,diabetes mellitus, hypertension, dyslipidemia (total cholesterol >220 mg/dl), and cardiovascular medication use (β-blockers, ACE-I, angiotensin-II receptor blockers, and spironolactone) was reviewed in medical records and charts. Patients with renal dysfunction (defined by creatinine ≥ 2.0 mg/dl) were excluded. One month after clinical condition being stable, standard ambulatory 24-hour electrocardiogram (ECG) recorders were placed on all participants. The ECG signals were sampled at 250 Hz and stored in SD memory card for offline analysis on a microcomputer. Subsequently, these patients were followed up and mortality or heart transplantation will be noted as end-point for follow-up. The Ethics Committee of National Taiwan University Hospital approved the study and all patients provided written informed consent.

Data pre-processing

Each digitalized 24-hour ECG data was annotated by an automated algorithm and the annotated file was then carefully inspected and corrected by technicians for extracting the RR intervals. The ectopic beats (including atrial or ventricular premature beats) were interpolated by its adjacent RR intervals. A four-hour period of RR intervals in daytime (between 9AM–5PM) was selected from each recording to avoid confounding effects on nonlinear or linear analysis caused by different sleep stage or diurnal rhythm [21,22]. Only subjects consisted of more than 80% of qualified normal sinus beats were included for further analysis (the typical RR-interval tracings and the corresponding recurrent plots for survival and mortality groups (Figure S1) as well as all of the RR-interval data are provided as supplementary materials (Materials S1)).

Time and frequency domain analysis

Standard deviation of normal RR intervals (SDNN) and percentage of absolute differences in normal RR intervals greater than 50 ms (pNN_{50}) were calculated to represent the total variance and vagal modulation of the HR. In addition, the spectrum analysis was carried out in accordance with the recommendations of the European Society of Cardiology and the North American Society of Pacing Electrophysiology [23]. The spectral density of each frequency band-high frequency (HF) (0.15–0.4 Hz), low frequency (LF) (0.04–0.15 Hz), and very low frequency (VLF) (0.003–0.04) were computed by average power spectrum.

Nonlinear methods

Nonlinear analysis enables the researchers to probe the fundamental characteristics of the signals. However, unwanted inferences such as noise and nonstationarity may introduce spurious features to the signals [24,25]. The underlying mechanisms of the irregular and unpredicted behavior of the signals can be misinterpreted and the reliability of the results of analysis can be compromised. Two methods had been chosen for their ability to evaluate the main properties of the signals [14,26].

Detrended fluctuation analysis (DFA)

DFA is a modified root-mean-square analysis used to evaluate the fractal correlation beneath the heart rate fluctuation originated from the interacted regulatory mechanisms. The algorithm has been described in detail elsewhere [14]. To briefly introduce this method, at first, it eliminates the environmental inferences by removing the linear-fitted "local" trend over different time scales ("box sizes") in an integrated time series. Next, the root-mean-square fluctuation of this integrated and detrended time series is calculated. This procedure is repeated over different time scales and then the slope of the curve (α exponent) can be estimated on the log-log plot of fluctuations versus box sizes.

In addition, a crossover phenomenon of α exponent in heart rate dynamics between short (4–11 beats) and long (11–64 beats) time scales has been proposed. The short-term (α_1) as well as long-term (α_2) fractal correlation exponents were calculated to provide better understanding of the fractal correlation property in physiological system [14].

MSE analysis

Instead of simply using single time scale to estimate the complex pattern (irregularity) of a time series, MSE extended this concept to evaluate the complexity of physiological signals on multiple time scales. It comprises of two steps: 1) coarse-graining the signals into different time scales; 2) quantify the degree of irregularity in each coarse-grained time series using sample entropy (SpEn) [27]. Finally, the entropy is calculated as a function of scale, providing a measure of information richness embedded in different time scales. In addition, it has shown that different features of small and large scales in different groups of subjects may assist the clinical categorization [19] and thus three different parameters were derived from the MSE profile: the summations of quantitative values of scale 1–5 ($Area_5$) or scale 6–20 ($Area_{6-20}$) which represent the complexity exhibit in short and long time scales, respectively; and the linear-fitted slope of the first 5 scales ($Slope_5$) (Figure 1). Although MSE was successfully applied in physiological signals [18,19,24], nonstationary artifacts especially trends can compromise the estimation of entropy-based analysis by increasing the standard deviation of the data. Hence, detrending process was used to attenuate the spurious influence caused by nonstationarity [24].

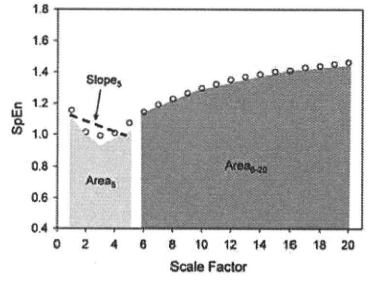

Figure 1. Demonstrative graph of MSE derived parameters. The profile of MSE can be assessed by a) its linear-fitted slope between certain scales which represent the complexity behaviors of the signals. The negative slope may indicate a random-like structure over certain timescale. B) the area under curve between certain scales that may represent its quantitative feature of the underlying physiological mechanisms in certain time scales (ex. area under scale1~5 may respond to the ability of respiratory sinus arrhythmia).
doi:10.1371/journal.pone.0018699.g001

In this study, the empirical mode decomposition (EMD) method was adopted as an adaptive filter to eliminate the oscillations slower than VLF range in the original R-R interval signals [28]. The data subsequently evaluated by the MSE analysis after detrending. This algorithm, instead of removing trend with *a priori* mathematical formulas such as linear or polynomial functions [14,29], could evaluate the hidden dynamics of heart beat fluctuations better [9,10,29].

Statistical analysis

For the independence of different nominal variables between groups, the chi-square test or Fisher exact test were performed. The continuous variables were represented as mean value ± SD and the normality of those variables was evaluated by using the Shapiro-Wilk test. Then, the Mann-Whitney U test or Student's t test was applied to the between-group comparison accordingly while the Wilcoxon sign test or Student's paired t test was calculated for the intra-group comparison. The receiver operating characteristic curve (ROC) was constructed by the sensitivity and specificity of the continuous variable in predicting the end-point. Area under the ROC curve (AUCs) gave an estimate of the overall discriminate ability. Furthermore, the most predictive indexes will be selected to seek the optimal cut point within the 30^{th} to 70^{th} percentile for all patients in 5^{th}-percentile step. The maximal hazards ratio and independent correlation of variables with event status (mortality) was determined by Cox regression analysis. Then, Kaplan-Meier event probability curves and log rank analysis of the dichotomized groups were obtained. The statistical significance was set at $p<0.05$.

Results

Characteristics of Patients

A total of 40 heart failure patients (30 males and 10 females) with a mean age of 56±16 years were enrolled and followed-up for 684±441 days. Twenty-five patients received β-blockers (either carvedilol or metoprolol). Carvedilol was titrated from 3.25 mg per day and metoprolol was titrated from 12.5 mg per day to maximal tolerable doses. Six patients died or received heart transplantation during follow-up period of this study. The demographic and clinical data were showed in Table 1. No clinical variable was significantly different between these two groups (with or without β-blocker therapy).

Table 1. The clinical characteristics between patients with and without using β-blockers.

Patient characteristics	β-blockers(−) (n = 15)	β-blockers (+) (n = 25)	*p* value
Age (years)	61.7±14.7	51.8±13.5	$p=0.073$
Male/Female	9/6	21/4	$p=0.158$
Heart rate (bpm)	86±13	87±15	$p=0.793$
LVEF(%)	33±12	35±14	$p=0.684$
Creatinine	1.07±0.25	1.18±0.35	$p=0.280$
Fasting sugar (mg/dl)	113±47	122±47	$p=0.573$
Triglyceride (mg/dl)	129±85	195±177	$p=0.189$
Cholesterol (mg/dl)	185±35	185±65	$p=0.988$
Hemoglobin (g/dl)	13.6±1.9	13.4±2.3	$p=0.712$
Uric acid (mg/dl)	8.9±3.2	7.1±2.6	$p=0.138$
NYHA functional class			$p=0.660$
I	2	4	
II	8	10	
III	5	9	
IV	0	2	
Body mass index	25.4±5.2	25.6±5.3	$p=0.929$
Etiology of heart failure			$p=0.924$
Coronary artery disease	6	11	
Non-coronary artery Diseases	9	14	
Hypertension	4	11	
Diabetes mellitus	6	10	
Medication			$p=0.845$
ACE-I/ARB	12	19	
Loop diuretics	10	18	
Digoxin	9	10	
Spironolactone	6	7	

A total of 40 heart failure patients (30 males and 10 females) were enrolled in this study. No clinical variable was significantly different between the patients with or without β-blocker therapy.
NYHA = New York Heart Association; ACE-I = angiotensin converting enzyme inhibitor; ARB = angiotensin receptor blocker.
doi:10.1371/journal.pone.0018699.t001

Effect of β-blockers on autonomic activities and its fractal properties

While the conventional HRV measurements showed no significant different between these two groups, $DFA\alpha_1$ showed significantly higher values ($p=0.014$) in patients with β-blocker treatment (Table 2).

Effect of β-blockers on the dynamical complexity assessed by the MSE analysis

There was no significant difference when any single sample entropy value of scales 1 to 20 was compared between patient groups with or without β-blockers. However, the value of $Slope_3$ was not only significantly lower ($p=0.028$) in patients without β-blocker therapy but also exhibit a negative value (Table 2).

Application of MSE in prognostic prediction

Among all parameters, $Area_5$, $Area_{6-20}$, and LF were significantly lower ($p=0.027$, $p=0.021$, and $p=0.004$ respectively) in the mortality group. (Table 3) Moreover, the ROC of the previously proposed predictors (LF, VLF, and $DFA\alpha_1$) and the new derived parameters ($Area_5$ and $Area_{6-20}$) were depicted in Figure 2. $Area_{6-20}$ (AUC:0.858±0.075) showed the best overall discriminative power than LF (AUC: 0.784±0.087), VLF (AUC:0.735±0.117), $DFA\alpha_1$ (AUC:0.71±0.145) and $Area_5$ (AUC:0.794±0.108) in mortality or heart transplant prediction. Therefore, $Area_{6-20}$ was adopted to perform the analysis of Kaplan-Meier survival curves. The value of $Area_{6-20} \leqq 21.2$ was a significant predictor of mortality or heart transplant (p = 0.0014). (Figure 3)

Discussion

Although the effects of β-blockers on HRV indices have been extensively studied [30–32], the effects of β-blockers on MSE are still unclear. The present study was the first study to assess the relationship between β-blockers and MSE in CHF patients. The main findings of this preliminary study were that the β-blocker therapy may change the short-term complexity (the slope of MSE between scale 1 to 5). But the most significant predictor of mortality or heart transplantation was the long-term complexity (the area under the MSE curve for scale 6 to 20). Therefore, we found an alternative prognostic predictor of CHF in addition to neurohormonal inhibition therapy by assessing the nonlinear characteristics of the heart rate fluctuations.

Table 2. Effect of the β-blockers on the autonomic activities, fractal properties and MSE.

	β-blockers(−) (n = 15)	β-blockers(+) (n = 25)	*p* value
Time domain analysis			
SDNN	53.2±17.8	49.1±26.9	$p=.332$
pNN_{50}	0.91±0.85	0.76±1.13	$p=.100$
Frequency domain analysis			
HF	31.43±20.91	27.9±35.3	$p=.088$
LF	56.3±43.0	90.9±102.9	$p=.659$
VLF	484.8±321.7	563.0±462.9	$p=.956$
Detrended fluctuation analysis			
α_1	0.91±0.22	1.10±0.34	$p=.014$
α_2	1.27±0.09	1.26±0.18	$p=.679$
Multiscale entropy			
$Slope_5$	−0.02±0.07	0.03±0.08	$p=.028$
$Area_5$	5.3±1.2	5.5±1.1	$p=.719$
$Area_{6-20}$	13.1±3.0	14.3±2.7	$p=.211$

While the conventional HRV measurements showed no significant different between these two groups, nonlinear indices, $DFA_{\alpha 1}$ and the value of $Slope_5$, were significantly lower in patients without β-blocker therapy.
$Slope_5$ = the linear-fitted slope of the first 5 scales, $Area_5$ = the summations of quantitative values of scale 1–5, $Area_{6-20}$ = the summations of quantitative values of scale 6–20.
doi:10.1371/journal.pone.0018699.t002

Table 3. Prognostic value of parameters of HRV.

	Survival group (n = 34)	Mortality group (n = 6)	*p* value
Time domain analysis			
SDNN	52.8±23.5	38.4±22.9	$p=.225$
pNN_{50}	0.88±1.09	0.46±0.37	$p=.939$
Frequency domain analysis			
HF	32.1±32.0	12.6±9.9	$p=.092$
LF	87.6±90.1	23.3±22.6	$p=.027$
VLF	575.4±420.4	297.4±290.5	$p=.071$
Detrended fluctuation analysis			
α_1	1.06±0.27	0.84±0.45	$p=.127$
α_2	1.28±0.13	1.15±0.23	$p=.239$
Multiscale entropy			
$Slope_5$	0.02±0.07	−0.03±0.11	$p=.197$
$Area_5$	5.6±1.0	4.5±1.1	$P=.021$
$Area_{6-20}$	22.3±3.5	16.3±4.5	$p=.004$

Among all parameters, $Area_5$, $Area_{6-20}$, and LF were significantly lower ($p=0.027$, $p=0.021$, and $p=0.004$ respectively) in the mortality group and those indices may potentially serve as outcome predictors.
$Slope_5$ = the linear-fitted slope of the first 5 scales, $Area_5$ = the summations of quantitative values of scale 1–5, $Area_{6-20}$ = the summations of quantitative values of scale 6–20.
doi:10.1371/journal.pone.0018699.t003

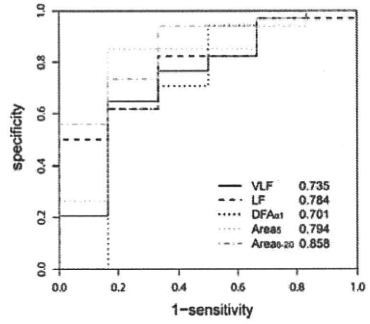

Figure 2. Very-low-frequency component (VLF; black, solid line), low-frequency component (LF; black, dashed line), short-term fractal exponent ($DFA\alpha_1$; black, dotted line), the summations of quantitative values of scale 1–5 ($Area_5$; grey, dashed line), and the summations of quantitative values of scale 6–20 ($Area_{6-20}$; grey, dash-dotted line) receiver operating characteristic (ROC) curves. The area under each ROC curves (AUC) was calculated for each parameters. The AUCs were 0.735 for VLF, 0.784 for LF, 0.701 for $DFA\alpha_1$, 0.794 for $Area_5$, and 0.858 for $Area_{6-20}$.
doi:10.1371/journal.pone.0018699.g002

Effect of β-blocker therapy on linear and nonlinear properties of HRV

All linear HRV measurement showed no difference between patients with or without β-blocker treatment in the present study.

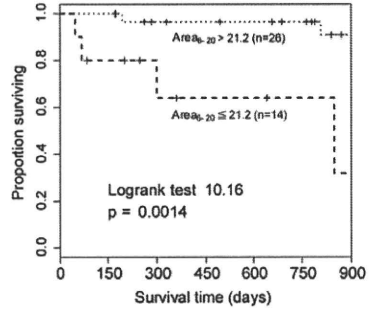

Figure 3. Using MSE $Area_{6-20} \leqq 21.2$ as a clinical predictor, significant difference in survival was noted from the Kaplan-Meier survival curve ($P=0.0014$).
doi:10.1371/journal.pone.0018699.g003

Other researchers have proposed that the restoration of autonomic function can be assessed by HRV indices [30,31,33]. The discrepancy between our finding and previous studies could be due to several factors. The first, the β-blockers were titrated according to patients' tolerance in our study. Therefore, the duration and dosage of β-blockers were variable. The second, the ECG was recorded 1 month after clinical condition being stable in our study. However, significant changes of most linear HRV parameters are found after 12 weeks of treatments. The short-term fractal scaling correlation index, $DFA\alpha_1$, was markedly higher in β-blocker group. The reversal of $DFA\alpha_1$ is also reported after administrating β-blocker in patients with CHF [33]. Our data showed similar results.

The new nonlinear method, MSE, allows us to evaluate the information richness in heart beat time series over different time scales. Although the underlying mechanisms responsible for the quantitative feature of the MSE in different time scales are still unclear, previous studies have shown that the complexity decreased significantly during aging and further deteriorated in patients with CHF [19]. We applied three different parameters, $Area_5$, $Area_{6-20}$, and $Slope_5$, to compare patients with or without β-blocker treatment. The summation of entropy values at different time scales may give the quantitative estimation of information richness over certain time scales. That is, $Area_5$ and $Area_{6-20}$ can probe the complexity structure of the heart rate dynamics in short (e.g., 1 to 5 heart beats) and longer (e.g., 6 to 20 heart beats) time scales, respectively. The $Slope_5$ also outlined the structure of heart rate dynamics in short time scale [19]. The negative value of $Slope_5$ indicates random-like patterns in short time scales. Therefore, the significant difference between β-blocker and non β-blocker groups might due to dysfunction of the short-term regulatory mechanisms coincided with the results assessed by $DFA\alpha_1$.

Complexity analysis as a prognosis predictor

Applying Fourier-based method to nonlinear or nonstationary signals may result in inaccurate estimations [9,29] and compromise the sensitivity of linear HRV measurements. Recently, $DFA\alpha_1$ has been proposed to be a better predictor for CHF patients [34]. In the present study, SDNN and $DFA\alpha1$ failed to predict the prognosis of CHF patients. Makikallio *et al.* noticed that HRV indexes such as SDNN is less sensitive in CHF patient with NYHA>III [35]. Sixteen patients (40%) were classified as NYHA III–IV in our study and five out of them were in mortality group. Moreover, administration of beta-blockade has shown a reversal effect in either linear and nonlinear parameters such as SDNN, HF, LF and $DFA\alpha_1$ [30,32,33]. Half of the patients with poor outcome were treated with beta blocker which may potentially influence the parameters. SDNN and $DFA\alpha_1$ may be, therefore, insensitive to predict their prognosis. $Arca_5$ and $Arca_{6-20}$ derived from MSE were markedly lower in the mortality group. This phenomenon was in agreement with those found by Costa *et al.* in MUSIC study [19]. Although the underlying mechanisms were still unclear, this preliminary study provided a new insight for the prognosis of CHF by probing the dynamical complexity on the system level. It could potentially offer an alternative marker for the outcome of CHF in addition to neurohormonal inhibition therapy.

Limitations of study

First, our study had small sample size and no placebo-controlled group. Second, all ECG data were recorded in normal "free-running" conditions with possible confounding factors (e.g., physical activities, different breathing patterns, and so on). The additive or dynamical noises may affect the properties of the signals. Although we examined and interpreted the results of the analysis cautiously and the differences characteristics of the patients were unlikely due to the noise, we did not assess the features or level of noise for more detailed information that may benefit the exploration of the underlying deterministic rules. Finally, some parameters related to possible physiological mechanisms of MSE were not collected, such as baroreflex sensitivity, catecholamine levels, and chemoreflex activities.

In conclusions, the area under the MSE curve for scale 6 to 20 is not relevant to β-blockers and could further warrant independent risk stratification for the prognosis of CHF patients.

Supporting Information

Figure S1 The 4-hour time tracings of RR intervals of survived patient (A) and patient who died after 1 year (B) and the return map traits of three-dimensional RR time series reconstruction (x-axis for RRn, y-axis for RR_{n+1} and z-axis for RR_{n+2}) of survived patient (C) and expired patients (D). Note that the trait of the map in survival patient was similar to that in expired patient.
(TIFF)

Materials S1 The RR intervals of each patient was output in a one-column Ascii file and categorized into two groups according to their outcomes after 2.5 years follow up. All of the files were packed into a compressed RAR file.
(RAR)

Author Contributions

Conceived and designed the experiments: YLH MTL. Performed the experiments: YHL CL. Analyzed the data: MTL CL. Contributed reagents/materials/analysis tools: YLH MTL. Wrote the paper: YLH CL.

References

1. Wang TJ, Evans JC, Benjamin EJ, Levy D, LeRoy EC, et al. (2003) Natural history of asymptomatic left ventricular systolic dysfunction in the community. Circulation 108: 977–982.
2. Stewart S, Jenkins A, Buchan S, McGuire A, Capewell S, et al. (2002) The current cost of heart failure to the National Health Service in the UK. Eur J Heart Fail 4: 361–371.
3. van Jaarsveld CH, Ranchor AV, Kempen GI, Coyne JC, van Veldhuisen DJ, et al. (2006) Epidemiology of heart failure in a community-based study of subjects aged > or = 57 years: incidence and long-term survival. Eur J Heart Fail 8: 23–30.
4. Flather MD, Yusuf S, Kober L, Pfeffer M, Hall A, et al. (2000) Long-term ACE-inhibitor therapy in patients with heart failure or left-ventricular dysfunction: a systematic overview of data from individual patients. ACE-Inhibitor Myocardial Infarction Collaborative Group. Lancet 355: 1575–1581.
5. Dahlof B, Devereux RB, Kjeldsen SE, Julius S, Beevers G, et al. (2002) Cardiovascular morbidity and mortality in the Losartan Intervention For Endpoint reduction in hypertension study (LIFE): a randomised trial against atenolol. Lancet 359: 995–1003.
6. Cohn JN, Tognoni G (2001) A randomized trial of the angiotensin-receptor blocker valsartan in chronic heart failure. N Engl J Med 345: 1667–1675.
7. Fauchier L, Babuty D, Cosnay P, Fauchier JP (1999) Prognostic value of heart rate variability for sudden death and major arrhythmic events in patients with idiopathic dilated cardiomyopathy. J Am Coll Cardiol 33: 1203–1207.
8. La Rovere MT, Pinna GD, Maestri R, Mortara A, Capomolla S, et al. (2003) Short-term heart rate variability strongly predicts sudden cardiac death in chronic heart failure patients. Circulation 107: 565–570.
9. Lo MT, Tsai PH, Lin PF, Lin C, Hsin YL (2009) The nonlinear and nonstationary properties in EEG signals: probing the complex fluctuations by Hilbert Huang Transform. Adv Adapt Data Anal 1: 461–482.
10. Peng CK, Costa M, Goldberger AL (2009) Adaptive data analysis of complex fluctuations in physiologic time series. Adv Adapt Data Anal 1: 61–70.

11. Goldberger AL, Amaral LA, Hausdorff JM, Ivanov PC, Peng CK, et al. (2002) Fractal dynamics in physiology: alterations with disease and aging. Proc Natl Acad Sci U S A 99 Suppl 1: 2466–2472.
12. Buchman TG (2002) The community of the self. Nature 420: 246–251.
13. Lombardi F (2000) Chaos theory, heart rate variability, and arrhythmic mortality. Circulation 101: 8–10.
14. Peng CK, Havlin S, Stanley HE, Goldberger AL (1995) Quantification of scaling exponents and crossover phenomena in nonstationary heartbeat time series. Chaos 5: 82–87.
15. Jagric T, Marhl M, Stajer D, Kocjancic ST, Jagric T, et al. (2007) Irregularity test for very short electrocardiogram (ECG) signals as a method for predicting a successful defibrillation in patients with ventricular fibrillation. Transl Res 149: 145–151.
16. Perc M (2005) Nonlinear time series analysis of the human electrocardiogram. European Journal of Physics 26: 757–768.
17. Perc M (2005) The dynamics of human gait. European Journal of Physics 26: 525–534.
18. Yuan HK, Lin C, Tsai PH, Chang FG, Lin KP, et al. (2011) Acute increase of complexity in the neurocardiovascular dynamics following carotid stenting. Acta Neurol Scand 123: 187–192.
19. Costa M, Goldberger AL, Peng CK (2005) Multiscale entropy analysis of biological signals. Phys Rev E Stat Nonlin Soft Matter Phys 71: 021906.
20. Costa M, Cygankiewicz I, Zareba W, Bayes de Luna A, Goldberger AL, et al. (2006) Multiscale Complexity Analysis of Heart Rate Dynamics in Heart Failure: Preliminary Findings from the MUSIC Study. Comput Cardiol 33: 101–103.
21. Pikkujamsa SM, Makikallio TH, Sourander LB, Raiha IJ, Puukka P, et al. (1999) Cardiac interbeat interval dynamics from childhood to senescence: comparison of conventional and new measures based on fractals and chaos theory. Circulation 100: 393–399.
22. Vanoli E, Adamson PB, Ba L, Pinna GD, Lazzara R, et al. (1995) Heart rate variability during specific sleep stages. A comparison of healthy subjects with patients after myocardial infarction. Circulation 91: 1918–1922.
23. (1996) Heart rate variability: standards of measurement, physiological interpretation and clinical use. Task Force of the European Society of Cardiology and the North American Society of Pacing and Electrophysiology. Circulation 93: 1043–1065.
24. Costa M, Priplata AA, Lipsitz LA, Wu Z, Huang NE, et al. (2007) Noise and poise: Enhancement of postural complexity in the elderly with a stochastic-resonance-based therapy. Europhys Lett 77: 68008.
25. Kantz H, Schreiber T (2004) Nonlinear Time Series Analysis. Cambridge: Cambridge University Press.
26. Costa M, Goldberger AL, Peng CK (2002) Multiscale entropy analysis of complex physiologic time series. Phys Rev Lett 89: 068102.
27. Richman JS, Moorman JR (2000) Physiological time-series analysis using approximate entropy and sample entropy. Am J Physiol Heart Circ Physiol 278: H2039–H2049.
28. Wu Z, Huang NE, Long SR, Peng CK (2007) On the trend, detrending, and variability of nonlinear and nonstationary time series. Proc Natl Acad Sci U S A 104: 14889–14894.
29. Lo MT, Novak V, Peng CK, Liu Y, Hu K (2009) Nonlinear phase interaction between nonstationary signals: a comparison study of methods based on Hilbert-Huang and Fourier transforms. Phys Rev E Stat Nonlin Soft Matter Phys 79: 061924.
30. Sanderson JE, Chan SK, Yip G, Yeung LY, Chan KW, et al. (1999) Beta-blockade in heart failure: a comparison of carvedilol with metoprolol. J Am Coll Cardiol 34: 1522–1528.
31. Mortara A, La Rovere MT, Pinna GD, Maestri R, Capomolla S, et al. (2000) Nonselective beta-adrenergic blocking agent, carvedilol, improves arterial baroflex gain and heart rate variability in patients with stable chronic heart failure. J Am Coll Cardiol 36: 1612–1618.
32. Sanderson JE, Yeung LY, Chan S, Tomlinson B, Kay R, et al. (1999) Effect of beta-blockade on baroreceptor and autonomic function in heart failure. Clin Sci (Lond) 96: 137–146.
33. Lin LY, Lin JL, Du CC, Lai LP, Tseng YZ, et al. (2001) Reversal of deteriorated fractal behavior of heart rate variability by beta-blocker therapy in patients with advanced congestive heart failure. J Cardiovasc Electrophysiol 12: 26–32.
34. Ho KK, Moody GB, Peng CK, Mietus JE, Larson MG, et al. (1997) Predicting survival in heart failure case and control subjects by use of fully automated methods for deriving nonlinear and conventional indices of heart rate dynamics. Circulation 96: 842–848.
35. Makikallio TH, Huikuri S, Kober L, Torp-Pedersen C, Peng CK, et al. (1999) Fractal analysis of heart rate dynamics as a predictor of mortality in patients with depressed left ventricular function after acute myocardial infarction. TRACE Investigators. TRAndolapril Cardiac Evaluation. Am J Cardiol 83: 836–839.

(Second presenter) C2010

In infant and children with bradycardia that unresponsive to oxygenation and/or ventilation (P), does the use of atropine (I), as compared with epinephrine (C), improve patient outcome return to age-appropriate heart rate, subsequent pulseless arrest, survival) (O)?

Worksheet identifier: Peds-052(B)
Author: Sasa Kurosawa, MD
Affiliation:
1) Research Inst., National Center for Child Health & Dev.
2) Shizuoka Children's Hospital
Taskforce: PEDS
Other Worksheet Authors: Susan Fuchs, Masahiko Nitta(042)

(Second Presenter) C 2010

Worksheet Specific Conflict Of Interest Disclosure

- Commercial/industry
  - none
- Potential intellectual conflicts
  - none

(Second presenter) C2010

Differences in COS Statement and Treatment Recommendation compared to first presenter

- *I almost agree with first presenter (Susan Fuchs).*

(Second presenter) C2010

Differences in supporting evidence

Summary of evidence

Evidence Supporting Clinical Question

	1	2	3	4	5
Good					
Fair					
Poor				Fullerton,1991(E)	

Level of evidence

A = Return of spontaneous circulation
B = Survival of event
C = Survival to hospital discharge
D = Intact neurological survival
E = Other endpoint
Italics = Animal studies

$ denotes key article(s)

(Second presenter) C2010

Differences in Neutral evidence

Summary of evidence

Evidence Neutral to Clinical Question

	1	2	3	4	5
Good					
Fair					Brady, 1999, (E) Smith, 1994, (E) Chadda, 1977, (E)
Poor				Zimmerman, 1986(E)	

Level of evidence

A = Return of spontaneous circulation
B = Survival of event
C = Survival to hospital discharge
D = Intact neurological survival
E = Other endpoint
Italics = Animal studies

$ denotes key article(s)

(Second presenter) C2010

Differences in Opposing evidence

Summary of evidence

Evidence Opposing Clinical Question

	1	2	3	4	5
Good				$Tibbals, 2006 (ABCD) $Guay, 2004 (ABCD) $Reis, 2002 (ABCD)	
Fair					
Poor					$Coon, 1981 (AC)

Level of evidence

A = Return of spontaneous circulation
B = Survival of event
C = Survival to hospital discharge
D = Intact neurological survival
E = Other endpoint
Italics = Animal studies

$ denotes key article(s)

(Second presenter) C2010

Differences in interpretation of Key studies

Key study #1 Reis, Pediatrics 2002

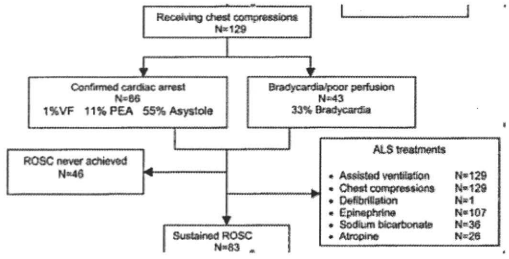

(Second presenter) C2010

Differences in interpretation of Key studies

Key study #2 Tibballs, Resuscitation 2006

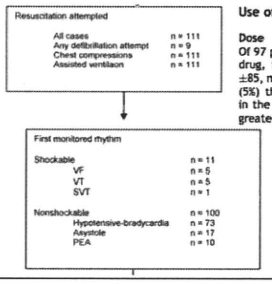

Use of adrenaline

Dose

Of 97 patients who received adrenaline as the first drug, the mean initial dose was 48 mcg/kg (S.D. ±85, median dose 12.5, range 1–441). In 5 patients (5%) the dose was <5 mcg/kg, in 50 (52%) it was in the range 5–15 mcg/kg and in 42 (43%) it was greater than 15 mcg/kg.

(Second presenter) C2010

Summary Of 3 In-hospital Arrest Studies (Tibballs, Guay, Reis)

Study	# pts	Rhythm	Epi used	Survivors
Tibballs	111	73 hypotension & bradycardia	97/111	38% at 1 yr
Guay	203	102 bradycardia	101/203	30% at 1 yr
Reis	129	43 bradycardia 86 arrest (55% asystole)	107/129 (atropine in 26)	33% brady at 24 hr 21 total to hosp d/c

(Second presenter) C2010

Differences in interpretation of Key studies

Key study #3 Coon, Ann Emerg Med 1981

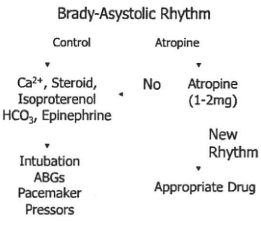

Fig.2. Protocol for treating brady-asystolic rhythm.

Table 3
PARAMETERS OF THERAPEUTIC EFFECACY

	Cobrol	Atropine Rhythm
	10/11	8/10
Pulse	6/11	4/10
Admit	2/11	2/10
Discharge	1/11	0/10

- Atropine may not affect the outcome of prehospital brady-asystolic cardiac arrest of primary cardiac etiology.

(Second presenter) C2010

Differences in interpretation of Key studies

Key study (Fuchs) Horigome, Acta Paediatrica Japonica 1993

- Atropine increased HR and mean blood pressure, but had no effect on left ventricular end diastolic dimension (LVEDD), or LV shortening fraction (LVSF).
- Myocardial depression caused by halothane was not improved by atropine

But I think if atropine increase HR and mBP, it is effective to improve systemic circulation.

(Second presenter) C2010

Different Consensus on Science statements

- Several adult studies and one pediatric study showed the efficacy of atropine for bradycardia caused by vagal stimulation, AV block, intoxication...(LOE 4, 5) [Brady, 1999, 47; Smith, 1994, 245; Zimmerman, 1986, 320; Chadda, 1977, 503].
- However, in pediatrics, bradycardia is mainly caused by hypoxia poor perfusion. Bradycardia is a pre-arrest state.
- Large pediatric Utstein studies demonstrated the significant frequency of hypotension-bradycardia, in pediatrics (LOE 4) [Guey, 2004, 373; Tibballs, 2006, 310; Reis, 2002, 200]. In this context, epinephrine is the first line drug rather than atropine.

(Second presenter) C2010

Different Treatment Recommendations

- There is no supportive evidence to demonstrate that atropine is superior to epinephrine in the case of bradycardia unresponsive to oxygenation and/or ventilation (excluding the case with vagal stimulation).
- Epinephrine is the first line drug for poorly perfused infants and children with bradycardia (heart rate <60 beats/min) that is unresponsive to oxygenation and/or ventilation.
  The first thing start chest compressions!

WORKSHEET for Evidence-Based Review of Science for Emergency Cardiac Care

Worksheet author(s)

Susan Fuchs, Sasa Kurosawa, Masahiko Nitta	**Date Submitted for review:** December 25, 2009

Clinical question.

Fuchs and Kurosawa: In infant and children with bradycardia that unresponsive to oxygenation and/or ventilation(P), does the use of atropine(I), as compared with epinephrine(C), improve patient outcome(return to age-appropriate heart rate, subsequent pulseless arrest, survival)(O)?

Nitta: In infants and children with cardiac arrest (out-of-hospital and in-hospital) or symptomatic bradycardia (P), does the use of atropine (I) compared with no atropine use (C), improve outcome (O) (eg. ROSC, survival)?

Is this question addressing an intervention/therapy, prognosis or diagnosis? Intervention
State if this is a proposed new topic or revision of existing worksheet:

Conflict of interest specific to this question

Do any of the authors listed above have conflict of interest disclosures relevant to this worksheet? No

Search strategy (including electronic databases searched).

Fuchs (052A):
Embase: bradycardia, atropine, epinephrine: 47 articles- none useful
Embase June 4, 2009: bradycardia, epinephrine, atropine : 11 articles from combined search-none useful, 21 from bradycardia and epinephrine- 1 useful-had already, 108 from bradycardia and atropine-1 useful-had already
Pubmed: bradycardia (mesh), atropine(mesh), atropine derivative(mesh), epinephrine(mesh) 31 articles results- none were useful
Cochrane library: bradycardia (mesh), epinephrine (mesh), atropine (mesh): 97 articles, 1 useful (epinephrine for the resuscitation of apparently stillborn or extremely bradycardic newborn infants AJA Zino, MW Davies, PG Davis Cochrane Database of Systemic Reviews 2002, Issue 3, Art no: CD003849.
Cochrane library June 4, 2009- no additional information that previously
Pubmed: bradycardia (mesh), atropine(mesh), atropine derivative(mesh), epinephrine(mesh) : 69 articles, 5 possibly useful

Hand searching references of articles
Review of 2005 ILCOR worksheets on similar topic
Recommendation from Dr Morley

Kurosawa (052B): Databases searched: Medline, ECC EndNote Master Library
Previous 2005 WS related to this question was reviewed and added several hand search.

#1 Bradycardia, Atropine, Child → hits 122
#2 Bradycardia, Epinephrine, Child → hits 25
#3 #1 OR #2 → hits 136 → 1 article(#1)
#4 Bradycardia, Resuscitation, Atropine → hits 81
#5 Bradycardia, Resuscitation, Epinephrine → hits 72
#6 #4 OR #5 → hits 119 → 4 article(#2 - #5)

#7 "Atropine"[Mesh] AND "Bradycardia"[Mesh] AND "Child"[Mesh] → hits 49
#8 "Epinephrine"[Mesh] AND "Bradycardia"[Mesh] AND "Child"[Mesh] → hits 5
#9 #7 OR #8 → hits 53, but there is no appropriate article.

#10 What is the optimal drug therapy for significant bradycardia?(WS91 Lim Swee Han, 20 Oct 2004) → 2 articles(#6, #7)
#11 Additional hand search → 2 articles(#8, #9)

Nitta (042B):
Databases searched: MEDLINE, Cochrane, ECC EndNote Master Library
Previous 2005 WS related to this question was reviewed and added several hand search.
#1 "Heart Arrest"[Mesh] AND "Atropine"[Mesh]
#2 "bradycardia"[Mesh] AND "Atropine"[Mesh]
#3 #1 or #2 advanced search child: 0-18 years
#4 #2 and (symptomatic bradycardia or resuscitation or shock or cardiopulmonary failure)

#5 "Heart Arrest"AND "Atropine"
#6 "symptomatic bradycardia" AND "Atropine"
#7 #5 or #6 advanced search child: 0-18 years
#8 Additional hand search

- **State inclusion and exclusion criteria**

Fuchs: None
Kurosawa: Included all human clinical trials, meta-analysis, case reports, guidelines.
English only.
Review articles and animal experiments were excluded.
Nitta: The following studies were excluded: Not true cardiac arrest cases.
Included all human clinical trials, meta-analysis, and animal experiments. English Language limitations.
Review articles were excluded.

- **Number of articles/sources meeting criteria for further review:**

Fuchs :12
Kurosawa: 9 articles relevant to the topic (from 308 hits and previous WS) were reviewed in detail
Nitta: • **Number of articles/sources meeting criteria for further review:**
#3 9 articles relevant to the topic (from 123 hits)
#1 17 articles relevant to the topic (from 183 hits)
#4 4 articles relevant to the topic (from 57 hits)
#7 9 articles relevant to the topic (from 85 hits)
#8 2 articles relevant to the topic
#3 or #1 or #4 or #6 or #8 22 articles relevant to the topic and 12 articles were reviewed in detail

Summary of evidence

Studies in **Bold**-Fuchs
Studies in Normal font-Kurosawa
Studies in *Italics*- Nitta
Studies in **Bold** and Underlined-Fuchs and Kurosawa
Studies in **Bold** & *Italics*- Fuchs and Nitta
Studies in *Italics* and underlined-Kurosawa and Nitta
Only study cited in all 3 (***bold, italics and underlined***)-Coon

Evidence Supporting Clinical Question

Good					*Blecic (AE)*
Fair					*Stiell (B)*
Poor			*Meaney (C)* *Reis (B)*	**Fullerton E (prevent recurrence of bradycardia) *** *Thrush (E)*	***Brown –A,B,C,E* (sinus rhythm)** ***Stuevan A*** *Sorensen (A)*
	1	2	3	4	5
	Level of evidence				

A = Return of spontaneous circulation
B = Survival of event
* Pediatric Study
C = Survival to hospital discharge
D = Intact neurological survival
E = Other endpoint
Italics = Animal studies

Evidence Neutral to Clinical question

Good					**Angelos A** ***Kaplan* B** **McCaul B**
Fair					**Chow E (histochemical studies)** **Brady (B,E)** Smith (E) Chadda (E) Oshige (BE) Niemann (A)
Poor				**Lienhart A *** Zimmerman (E) McNamara (E) Polin (E) Sacchetti (e) Rothrock (E)	**Iseri AC** **Steuvan C** Yilmaz (E) *Redding (A)*
	1	2	3	4	5
	Level of evidence				

A = Return of spontaneous circulation
B = Survival of event
* Pediatric Study
C = Survival to hospital discharge
D = Intact neurological survival
E = Other endpoint
Italics = Animal studies

Evidence Opposing Clinical Question

Good	**Horigome E ***			Tibballs (ABCD) Guay (ABCD) Reis (ABCD)	*DeBehnke (A)* ***Coon (ABCE)***
Fair					
Poor			*Herlitz 1994 (BCE)* *Herlitz 2003 (BCE)* *Engdahl (BCE)*		
	1	2	3	4	5
	Level of evidence				

A = Return of spontaneous circulation
B = Survival of event
* Pediatric Study
C = Survival to hospital discharge
D = Intact neurological survival
E = Other endpoint
Italics = Animal studies